IEEE Access
Multidisciplinary | Rapid Review | Open Access Journal

SPECIAL SECTION ON DIGITAL TWINS FOR ENERGY-RELATED APPLICATIONS

Received 12 March 2026, accepted 25 March 2026, date of publication 3 April 2026, date of current version 9 April 2026.

Digital Object Identifier 10.1109/ACCESS.2026.3680461

RESEARCH ARTICLE

Glow Plug Integrated Solar Heater for Reducing Initial Waiting Period of Evaporation Lag and Improve Thermal Efficiency in Solar Still Desalination

SYED ZAHURUL ISLAM[1], **(Member, IEEE)**, **ASMARASHID BIN PONNIRAN**[1], **(Member, IEEE)**, **MOHAMMAD RASHED M. ALTIMANIA**[2], **KHALED SALEEM S. ALATAWI**[2], **FAHAD M. ALMASOUDI**[2], **AMIMUL AHSAN**[3,4], **MOHAMMAD LUTFI OTHMAN**[5], **(Senior Member, IEEE)**, **AND JASIM UDDIN**[6], **(Member, IEEE)**

[1]Faculty of Electrical and Electronic Engineering, Universiti Tun Hussein Onn Malaysia, Parit Raja, Johor 86400, Malaysia
[2]Department of Electrical Engineering, Faculty of Engineering, University of Tabuk, Tabuk 71491, Saudi Arabia
[3]Department of Civil and Environmental Engineering, Islamic University of Technology (IUT), Gazipur 1704, Bangladesh
[4]Department of Civil and Construction Engineering, Swinburne University of Technology, Melbourne, VIC 3122, Australia
[5]Advanced Lightning, Power and Energy Research (ALPER) Centre, Faculty of Engineering, Universiti Putra Malaysia, Serdang, Selangor 43400, Malaysia
[6]EM-RFMic Engineering Group, Cardiff School of Technologies, Cardiff Metropolitan University, CF5 2YB Cardiff, U.K.

Corresponding author: Syed Zahurul Islam (zahurul@uthm.edu.my)

This work was supported by Universiti Tun Hussein Onn Malaysia (UTHM) through Tier 1 under Grant Q375.

ABSTRACT The current solar desalination process is facing a challenge of longer time for the brine temperature to reach the evaporation threshold during the winter with cooler ambient temperature, cloudy, and the initial hours of the day. This study aims to address the challenge by reducing initial waiting period of evaporation lag through integrating a glow plug enabled solar powered water heater (SPWH), operates at low resistance (0.48 – 0.81 Ω) and high power (12 V, 25 A, 300 W). Prior to implementation, mathematical modelling is employed to determine the appropriate sizing of the PV system, battery, cable, and maximum power point tracking (MPPT) controller. The results demonstrate a significant increase in the temperature of the brine, reaching 79.2 °C within 45 minutes at a rate of 0.96 °C/min. The temperature profile demonstrates that the brine water, reaching a steady peak with minimal fluctuations of ± 2 °C, retains heat more effectively than the chamber temperature due to its higher specific heat capacity. Throughout the experiment, the average brine temperature is maintained at 70.58 °C, even on a day with heavy cloud cover (average irradiance 418 W/m^2). Another noteworthy finding is that the system can produce more than 3.35 kg/m^2 of freshwater per day with the highest thermal efficiency of 68.18% under cloudy ambient conditions. The electrical performance of the system proves to be highly stable, with the voltages of both the PV system and battery experiencing minimal fluctuations not more than 0.9%. In addition, the system has achieved a cost-effective production rate of $0.09/kg. By employing this technique, challenges related to limited access to clean drinking water, scarcity of freshwater sources, and water quality issues in remote Malaysian islands can be effectively overcome.

INDEX TERMS Glow plug, solar heater, solar desalination, evaporation lag.

The associate editor coordinating the review of this manuscript and approving it for publication was Enrico Zio.

I. INTRODUCTION

Water, a naturally circulating resource, undergoes continuous replenishment; however, its usable form remains limited despite its critical importance to all life on Earth. Saline water, which constitutes most global water resources, is unsuitable for consumption or irrigation without treatment. In fact, only about 0.001% of the Earth total water volume is readily accessible in the atmosphere for direct use [1]. Solar desalination has emerged as a promising solution, utilizing solar radiation that penetrates a transparent top cover of a chamber to heat brine water. As solar energy is absorbed and transferred to the saline water, its temperature—and consequently its vapor pressure—increases, leading to evaporation and subsequent condensation on the cooler top cover surface [2], [3], [4]. Brine water desalination has become a key commercial method for producing freshwater, particularly in arid regions such as the Middle East and North Africa. More recently, certain Southeast Asian regions, notably Sabah in Northern Borneo, Malaysia, have also faced escalating freshwater scarcity due to rising demand, inadequate supply systems, mismanagement of river basins, and rapid population growth. These challenges are exacerbated by climatic variability driven by the southwest monsoon season, which frequently results in prolonged droughts and further threatens water security in the region [5].

To address this water crisis, few distillation methods have been developed for water desalination technology. Among these, solar distillation is one of the best practical and economical methods of freshwater production. Previous research indicates that around 1 m^2 of ground produces 3-4 L/day of freshwater. Because of the low volume, various studies have been conducted to improve the efficiency of solar stills by altering the design, incorporating additional effects such as multistage evacuated stills, and adding wicking material [4], [6]

Other utilized methods include thermal distillation [2], membrane separation [3], freezing and electrodialysis [7]. In the thermal distillation system, a concept involving a 1.0 m^2 absorber plate with a heat exchanger is introduced to enhance the evaporation rate. This system involves pumping warm water from the top of the sea and cold water from the bottom into the system [2]. The researcher in question leverages both solar and ocean thermal energy, achieving a freshwater production rate of 1.21 kg per hour. The initial investment cost amounts to US$ 434.00, although the electric cost of the water pump is not factored into this analysis. Membrane distillation is identified as an emerging desalination technology that effectively integrates both indirect and direct utilization of solar energy. Membrane distillation is a thermally powered technology driven by membranes that can operate across a wide range of input temperatures. Over the past two decades, scholars have undertaken theoretical and practical investigations into desalination systems incorporating solar-powered membrane distillation [3], [8], [9].

Few distillation methods have been developed for water desalination technology and solar distillation appears as one of the best practical and economical methods of freshwater production. For solar distillation, the basin solar still represents its simplest application. Previous research experience proves that around 1 m^2 of ground produces 3-4 L/day of freshwater. Because of the low volume of freshwater production, various studies have been done to improve the efficiency of solar stills by altering the design, incorporating additional effects such as multistage evacuated stills, and adding wicking material [4].

Researchers have introduced other improvements in different countries. The stepped solar still and twin wedge solar still in India produce 0.3 L/hour and 3.61 L/day, respectively [10], [11], phase change material attains 0.357 L/h in Sudan [12], [13] and marble stones yields 5.5 L/h in India, inclined cascade solar still produces 1.5 L/h in Morocco [14], [15], successive evaporation condensation solar still methods in Egypt can produce 5.2 L/m^2 [16], monolithic solar stills proposed for thermal improvement [17], compound parabolic concentrator tubular solar stills harvests 7.7 L/day [18], regression model analysis to predict the production of distilled water [19], and computational fluid dynamics model and investigation to improve by 30% [20].

Farooq et al. used solar air heater to increase the temperature of induced air in the humidification chamber [21]. This technique increased the temperature in the chamber faster. The results showed that 1.3 L/m^2 of water was produced at a flow rate of 0.017 kg/s in 9 h. Another research proposed a hemispherical solar still design to increase the productivity of freshwater [4]. The results indicate a rise in freshwater production from 2.8 L/m^2 to 4.2 L/m^2 per day with hemispherical solar still design compared to the normal design. A new triangular solar still shape, designed by Ahsan et al. is claimed to have a higher production rate and achieves 4.75 L/m^2 of freshwater per day [22]. The research shows regression analysis between sunlight heat energy and daily distillate output, humid air temperature, and daily distillate output. Razqin et al. proposed a double slope method using two materials - glass and plastic in their research [23]. The result found that the plastic solar still had a three times higher production per day and as it produced 2.01 L/m^2 of distilled water, opposed to 0.6 L/m^2 from the glass still. This can be concluded that plastic solar still is more efficient than glass material. Yahya et al. used thermal energy to heat water so that the effectiveness of solar heating system is used [24]. The goal was to reach the temperature of 70 ^oC on the temperature gauge. The temperature kept on rising each hour until the system reached its highest temperature of 62 ^oC at 13:00. By applying solar thermal energy, the maximum temperature was reached to 60 ^oC. In Tamil Nadu, researchers conducted experiment taking a twin wedge solar still by controlling temperature using sensing technology. From the six days experiment at 29-31 ^oC of ambient temperature and 721- 810 W/m^2 of solar irradiance, daily production of freshwater was 3.28 – 3.61 L/m^2 [11].

A research team conducted extensive studies on the shape and material of solar still, such as prismatic-shaped, hemispherical solar distillers, and dome-shaped solar distiller. In [25], a conventional and double-sloped solar distiller with two adjacent sprayers and a wicking prism container were compared and found that the double-sloped solar method can produce 7.94 kg/m^2/day compared to conventional type (5.31 kg/m^2/day). Furthermore, the improved system demonstrated better performance in terms of daily efficiency, achieving an increase of 3.8%. The study also introduced an LSTM (Long Short-Term Memory) model to predict freshwater output based on environmental input parameters. However, since these parameters are highly dependent on fluctuating climatic conditions, the model does not fully resolve the inherent intermittency and unpredictability of solar energy availability.

In [26], four different sizes of spherical rock salt balls (0.50, 1.0, 1.50, and 2.0 cm) were introduced into the saline water basin of the solar distiller for improving thermal performance. The use of these thermal storage elements resulted in brine temperatures that were approximately 0–11 ^{o}C higher than those in conventional systems, with peak temperatures reaching up to 65 ^{o}C, while the internal chamber temperature remained below 55 ^{o}C under ambient temperature of 45 ^{o}C and solar irradiance of 1000 W/m^2. The experimental outcomes demonstrated that freshwater production using the rock salt balls in the hemispherical solar distiller achieved yields of 6.77, 6.25, 5.92, and 5.67 kg/m^2/day corresponding to the respective ball sizes - substantially outperforming the conventional design, which produced only 4.65 kg/m^2/day. The hemispherical solar distillers are improved by adding metamorphic fabric materials, which can produce 7.60 kg/day·m^2 under the same ambient condition [27]. For using the PCM and CuO/water NF within the hemispherical distiller, the basin water temperature increases to 70 ^{o}C and internal chamber temperature of 60 ^{o}C at ambient temperature of 50 ^{o}C. The total freshwater production is 8.65 kg/m^2·day for using this technique [28]. As part of the improvement of the system, dome-shaped solar distillatory with a fountain feed supply and nanocomposite (DSD-FFS + NCPCM) is tested and showed that the daily product output is 7.21 kg/day/m^2 under the similar weather condition [29]. At 800 W/m^2 and 44 ^{o}C of ambient temperature, dome-shaped solar distiller is claimed to produce 9.27 kg/m^2/day of freshwater [30].

In the study [31], a heating plate powered by grid electricity was installed beneath the sprayed water outlet. The copper heating plate (40-60 W) was maintained at a temperature close to 100 ^{o}C, resulting in high electrical power consumption and increased operational cost. Solar energy concentration was achieved using a Fresnel lens integrated into the vaporization chamber. The experiments were conducted under bright summer conditions, with an ambient temperature of approximately 28 ^{o}C and peak solar irradiance reaching 1000 W/m^2. However, the study did not address the morning thermal lag, nor did it consider system performance during low irradiance conditions. In addition, the electrical characteristics and energy efficiency of the copper heating plate were not discussed. Since it is a hybrid system and copper plate is powered from grid, the proposed system is not suitable for remote applications. Similarly, another study [32] employed an auxiliary interfacial heating element to mitigate low irradiance conditions. Although this approach improved freshwater productivity, the experiments were conducted under relatively high solar irradiance levels ranging from 600 to 900 W/m^2, with an average saline water temperature of 30 ^{o}C and relative humidity between 35.6% and 72.6%. The system utilized a 150 KW_p solar PV module coupled with a 100 Ah battery; however, design specifications, system sizing calculations, and performance justification were not provided. Furthermore, the relationship between heater capacity, PV size, and battery storage was not analyzed, and relevant safety considerations were not discussed. In [33], the experiments were conducted in Portugal with the objective of assessing year-round applicability for small remote islands. The lowest freshwater productivity values of 0.45, 0.50, and 1.77 L/day-m^2 were reported during June–September 2021, August 2022, and February 2023, respectively. Although electrical heating was incorporated into the system, detailed specifications of the heating element and its operational performance were not provided. Moreover, no quantitative analysis was presented to evaluate the impact of auxiliary heating on system performance.

Moreover, the maximum temperature of the chamber of almost all these researchers could attain not more than 70 ^{o}C, which is not sufficient temperature for fast evaporation. Some research proposed air blower to harvest 30 L/m^2 [34] and further solar heater to produce up to 65 L/m^2 [21], however the cost of the systems is tremendously increased. Some researchers have emphasized the importance of both the design and materials of the solar still, as improvements in these aspects can significantly enhance production. However, there seems to be a disregard for appropriate sizing of the PV panels, batteries, and other related components used as power sources, along with adherence to electrical standards. Moreover, cloud cover in many countries is significantly high, causing fluctuations in solar irradiance. To mitigate this effect, proper design of PV-integrated battery management can provide a solution to manage dynamic changes in solar power harvesting.

After reviewing various studies aimed at improving solar still performance, the following research gaps were identified.

- At initial and late afternoon of the day (before 10:00 AM and after 3:00 PM), amount of vaporization is significantly low because it requires time to till the chamber temperature reaches to a certain level for evaporation. However, all previous studies reported that both brine and chamber temperatures have remained below 48 ^{o}C at this hour due to lower than 500 W/m^2 irradiance. This results in a low freshwater yield ranging from 0 to 0.4 L/m^2·h. This variation contributes to a significant decline in daily water production and overall system efficiency. Moreover, the existing enhancement techniques have limited effectiveness during these low-radiation periods, as they do not adequately address the drop in performance during early morning and late afternoon. In contrast, the climate in Southeast Asia possesses average daily ambient temperatures ranging from 21 - 32 °C and solar irradiance around 600 W/m^2. Therefore, the reported structural improvement techniques are not effective under this climate.

- When evaluating ambient conditions such as temperature and solar irradiance, most of the studies conducted in the Middle East and Egypt during the summer season. During this period, ambient temperatures typically exceed 45 °C, and solar irradiance reaches up to 1000 W/m^2 between 10:00 AM and 3:00 PM, which supports a faster evaporation process and high freshwater yield. In contrast, ambient temperature during winter months falls below 20°C. Consequently, no experimental investigations have been reported for winter conditions, limiting the understanding of system performance under low-temperature and irradiance scenarios.
- In addition, several studies have introduced auxiliary heating elements without providing a detailed discussion of their electrical characteristics. In such systems, the solar PV and battery sizing have been selected without clear design specifications or systematic sizing calculations. Moreover, these studies do not explain the selection of heater capacity in relation to system efficiency, PV module size, battery capacity, nor do they provide the corresponding performance analysis or address relevant safety standards. No analytical model has been presented that considers sizing factors, days of autonomy, in relation to the energy requirements of the heating element.

Based on the identified research gaps, the objectives are formulated to address the limitations of the existing system. The first objective is to design and model a solar powered water heater (SPWH) integrated with a glow plug to improve thermal efficiency by reducing the initial waiting period for evaporation, typically between 7:00 AM and 10:00 AM. Then, the second objective is to analyze the impact of utilizing a glow plug on the evaporation rate and yield in desalination process, with a specific focus on expedited evaporation.

The novelty of this study is to introduce a glow plug enabled SPWH, which operates at a very low-resistance (0.48 – 0.81 Ω) and functions as a very high-power DC heating element to rapidly raise the brine temperature. This new approach investigates the reduction in evaporation lag at low irradiance conditions, specially during the winter season. To the best of our knowledge, no study was conducted to overcome the problem when the solar irradiance and ambient temperature are < 500 W/m^2 or < 25 °C, respectively. The key contribution of this study lies in modelling and analysing the electrical aspects of integrating a glow-plug enabled SPWH, whereas most existing studies primarily focus on heater usage and chamber design without addressing

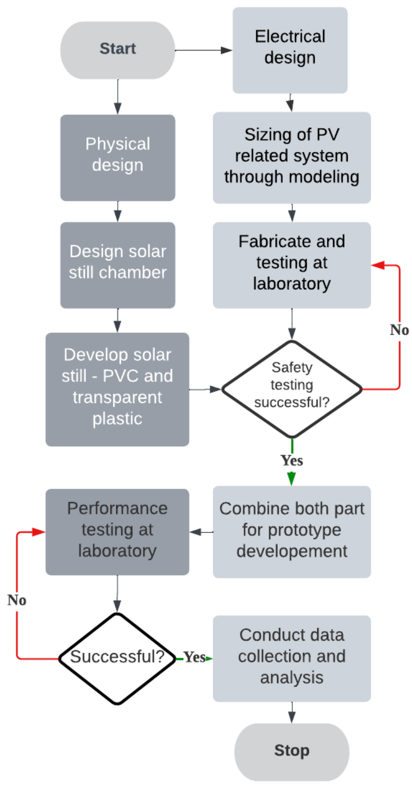

FIGURE 1. **Integrated system implementation flow diagram: physical and electrical design of single solar still chamber. Physical design ensures proper solar still chamber, while electrical design ensures safety and appropriate sizing of electrical components.**

the electrical part in detail. The hypothesis of this study is that utilizing a glow plug as a DC heater, characterized by low electrical resistance and high initial power output, can significantly reduce the time required for brine to reach evaporation temperature. This behavior is based on the principle that maximum electrical power is delivered at lower brine temperature due to the minimal resistance of the glow plug. As the brine temperature increases, the electrical resistance of the glow plug rises, resulting in a reduction in current and, consequently, a decrease in power. This effect is quantified by comparing the thermal response, freshwater yield, and system efficiency with those of a matched control system operating under identical environmental conditions.

This research makes a significant contribution by developing a self-contained PV system that reliably supplies ample power to support the proposed SPWH system. This ensures consistent evaporation rates throughout the day, regardless of fluctuations in solar irradiance. Furthermore, the system enables dual utilization of solar energy by converting it into heat for the desalination process. In the design process, careful consideration is given to the sizing of the PV array and battery bank. This involves analysing solar radiation data specific to the location, load demand, PV module manufacturing specifications, and battery requirements. These calculations and assessments collectively contribute to a well-designed and efficient system in compliance with IEC standards.

II. MATERIALS AND METHOD

This research aims to minimize the initial waiting period necessary for vaporization initiation, while concurrently attaining a brine temperature at approximately 80 °C to ensure consistent evaporation during periods of intermittent irradiance. For this purpose, a SPWH using a glow plug is proposed as an additional heating element.

For this purpose, the implementation of the single solar still prototype is explained by dividing into two parts, namely physical design of solar still and electrical system, as shown in Fig. 1. The physical structure of single solar still chamber is designed using low-cost PVC frame with transparent plastic cover, adapted from our previous research in modified form [6], [35]. In the design of electrical system, the sizing of solar PV, battery, and solar charger controller are determined from mathematical modeling and also adopted from our previous research [36], [37], [38]. Following the design specifications, the components are procured from a local supplier and subsequently fabricated within the laboratory environment. This ensures that the circuit can be operated safely and in accordance with proper measures. By combining the solar still and electrical parts, we tested again in the laboratory to ensure that any overcurrent flow from the battery to the glow plug can be safely triggered off by the switch. For this testing, a power supply is used to replace the PV panel. Adherence to recommended standards and codes ensures that the wiring sizes and materials can safely handle currents up to 30 A without the risk of overheating. We have also ensured that all wires, cables, and connections are properly insulated and rated for the current level to prevent electrical shocks and short circuits. During the testing, we periodically inspect and maintain all electrical components, connections, and devices in case any fault occurs. Once the testing is successfully completed, we conducted the experiment in an outdoor actual environment, replacing the power supply with PV panel. Drawing from our prior research [39], the meteorological data indicates that Malaysia experiences a consistent climate characterized by predictable weather, with year-round heat and humidity, and minimal fluctuations in temperature. It also describes very mere difference in ambient temperature, such as June (28 °C) and July (27.7 °C). Some researchers describe Malaysia as 'mere distinctive season country' and its climate is average and humid. Due to similar indices, we considered one-day data on an average cloudy day to analyze the performance of the system and the evaporation rate for peninsular Johor Malaysia.

A. CHARACTERISTICS OF GLOW PLUG

The glow plug is widely used in diesel engines during cold start, employing a structure based on resistive heating [40], [41], [42]. It is a straightforward method that eliminates the need for external electronic components. The hot surface heats its surroundings, expediting the evaporation of liquid diesel fuel and facilitating the ignition of the fuel-air mixture during engine startups in low ambient temperatures. Building on this principle, we tested incorporating the glow plug into solar stills, particularly during the initiation of the desalination process. This proposal is grounded in the understanding that the morning period typically features cooler ambient temperatures due to reduced irradiance. Unlike a conventional solar heater, the temperature of the heating element can rapidly exceed 1000 °C (eg. BERU, HKT, DENSO etc.) within 2-5 s when the glow plug is activated using a power supply.

The glow plug is 95mm long and operates at 12 or 24 V, depending on the accumulator voltage level shown in Fig. 2. Typically, the connecting bolt is linked to the positive power, while the body through part B is oriented to allow the current flow. Inside this part, there is a resistance, called 'resulting coil' which is responsible to limit the current flow and prevent the 'heating coil' from melting temperature. An insulating disc separates the positive and ground conductive bodies. The presence of the 'insulating coil' is crucial, given that the resistances involved are higher than those of non-insulated plugs. A high current flows through the resulting and heating coils, ultimately reaching the end of the heating coil within the body. Part A, the heating coil, is shorter than that of 'resulting coil' to keep the total resistance of these two coils low. This allows the heating coil to reach its maximum temperature within a short period of time.

In laboratory experiment, we investigated the behaviour of current, voltage, and resistances of the glow plug with temperature increase (Fig. 3). Since resistance is the ratio between voltage and current, the resistance of the glow plug increases temporality (initial resistance is 0.48, and then increase up to 0.81 Ω), meaning the current from the battery begins to drop. The min, max, and average resistances are found to be 0.48, 0.91, 0.76 Ω, respectively. Temperature reaches over 1000 °C in 5 s and remains almost constant. After a while, the resistance levels off, and the current flow is restricted to 6.8 A.

During increasing temperature, the resistance of the heating coil is proportional to the temperature (T) and the resistance (R). Resistance at final temperature (R_f) can be calculated using Eq. 1 and Eq. 2.

$$\begin{cases} R = kT \\ \dfrac{R}{T} = k \\ \dfrac{R_i}{T_i} = \dfrac{R_f}{T_f} \end{cases} \tag{1}$$

$$R_f = \frac{T_f \times R_i}{T_i} \tag{2}$$

In Eq. 1, k refers to a constant. If initial temperature, $T_i = 20\,^{\circ}\text{C}$, and final temperature, $T_f = 1000\,^{\circ}\text{C}$, R_f can be found as $5R_i$, which is 5 times of initial resistance (R_i). When the glow plug is directly connected to the battery, a maximum of 25 A current can flow, which can shorten the battery life.

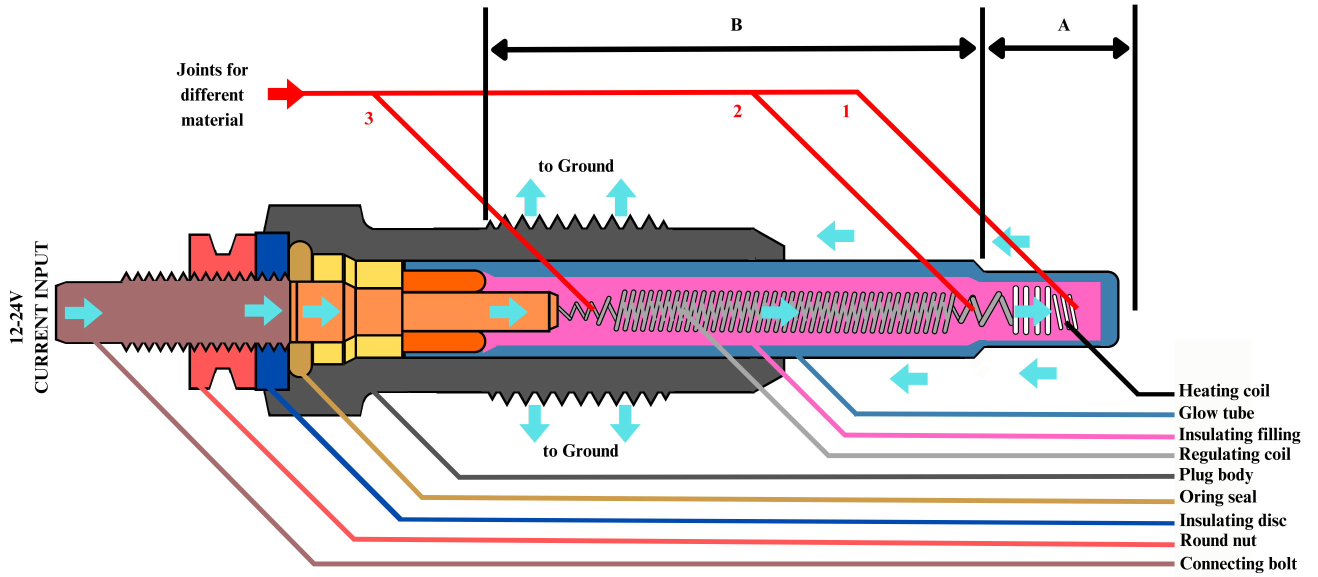

FIGURE 2. Physical structure of glow plug. It has two parts: Part A and Part B, with Part A containing a shorter coil to maintain low total resistance. This design enables the heating coil to reach its maximum temperature quickly.

B. ELECTRICAL SYSTEM DESIGN

The design of the electrical system is based on load power. The load, 300 W as a glow plug is the main heating element in this system. It has two parts- the upper body (73 mm) and the bottom tip (22 mm). The circuit diagram showing the connection of the glow plug to the MPPT charge controller is illustrated in Fig. 4, where both PV and battery are linked to the MPPT. The positive and negative terminals are separated by an insulated black ring placed between them. To avoid arcing, fiction, and heat loss, hexagonal flange nuts, washer, and cramp connector terminals were used for strong electrical connection between cable and glow plug. The Aluminum composite is engineered with precision, ensuring that only the heating element of the glow plug is immersed in the brine, while the remaining portion remains insulated from water to prevent any potential short circuits.

In order to find the required time (t) for reaching the brine temperature from the initial temperature (T_i) to the final temperature (T_f) °C, we adopted a model equation, shown in Eq. 3 by assuming that there is no loss of energy during this process.

$$t = \frac{m \times S_b \times (T_f - T_i)}{P_{load}} \tag{3}$$

Eq. 3 represents the energy needed for raising the temperature of m kg of brine from T_i to T_f °C. To accomplish this, t s time is required when utilizing a load power of P_{load} (W) to convert electrical energy into heat. S_b refers to the specific heat of the brine at 31 °C, measured as 4153.0 J/kg.K [43].

Based on the model equation above, the glow plug $P_{load} =$ 300 W is capable of increasing the 4.5 kg of brine water from 35 to 80°C temperature in 2803 s or 46.72 minutes. In this process, approximately 840.98 kJ of energy will be converted from electrical energy to heat. In practice, there is a loss of energy due to the design of the solar still and external heat can propagate into the chamber from the sunlight. Since it is powered by a PV powered battery, the size of the PV, battery, and MPPT charger is calculated prior to its development.

C. CABLE SIZING

To choose the suitable wire for the whole system, we have determined the Voltage Drop Index, VDI using Eq. 4.

$$VDI = \frac{I_{max} \times L}{V_{drop} \times V_{sys}} \tag{4}$$

Here, I_{max} and L refer to maximum current of the system and distance of the cable in feet, 25 A and 4.0 feet, respectively. V_{drop} (%) refers to voltage drop of the system and assuming was made to consider 2% acceptable voltage drop for this load. It is because conductors in electrical systems should not be sized with voltage drops exceeding 3%. V_{sys} denotes the voltage of the system, that is 12 V. This yields $VDI = 4.16$ from Eq. 4. Referring to the standard of the cable sizing based on VDI value, a 12 AWG copper conductor (cross-sectional area ≈ 3.31 mm^2) was selected for the system. The cable is rated for 90 °C insulation temperature and installed following standard extra-low voltage DC wiring practices. A high-temperature, ultra-flexible silicone-insulated tinned copper cable was used to ensure reliable electrical conductivity and thermal resistance under operating conditions. To ensure safe operation, the cable routing was kept short to minimize voltage drop and resistive power losses. In addition, appropriate overcurrent protection was

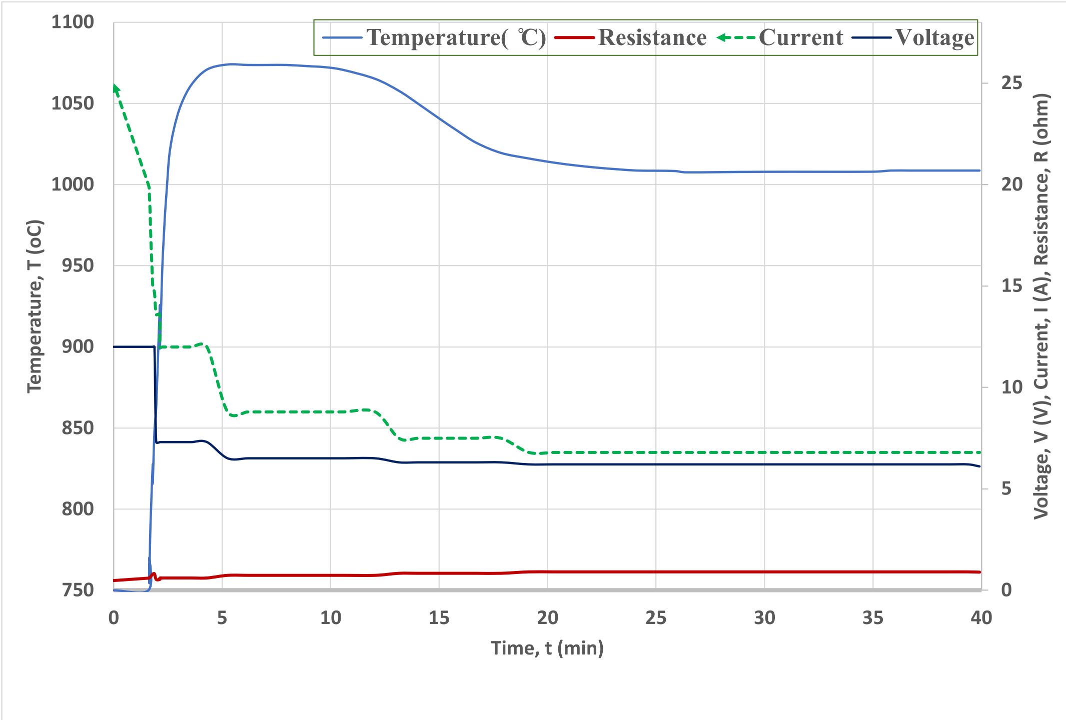

FIGURE 3. Characteristic of the glow plug: current, voltage, and resistance against temperature. Resistance can be obtained from the ratio of voltage and current, which shows that min and max resistances are 0.48 and 0.91 Ω, respectively.

implemented through a DC protection switch to safeguard the conductor and connected components under fault conditions. This configuration provides adequate current-carrying capacity, thermal stability, and safe operation of the PV-battery system.

D. PHOTOVOLTAIC (PV) PANEL SIZING

To determine the optimum size of PV, we can derive a set of model equations for the SPWH, shown in Eqs. 5,6,7, and 8. The electrical sizing equations are adopted from our previous publication, [44].

$$E_{load} = P_{load} \times h_{load} \tag{5}$$

$$E_{pv} = E_{load} \times 1.3 \tag{6}$$

$$P_{pv,peak} = \frac{E_{pv}}{S_h} \tag{7}$$

$$N_{pv} = \frac{P_{pv,peak}}{P_{max}} \tag{8}$$

Here, E_{load}, h_{load}, E_{pv}, $P_{pv,peak}$, N_{pv}, S_h, and P_{max} refer to load energy (W-h), daily load hour (h/day), total energy required from PV (Wh/day), required watt-peak size of PV (W), required number of PV panels, sun hour (h) and maximum power of PV (W) at Standard Test Conditions (STC), respectively. Eq. 5 determines the total watt-hour of the system load by multiplying load power and daily operation hours. In Eq. 6, we assume to be 30% system loss, which indicates multiplying by 1.3 with the total watt-hour of the load. In Eq. 7, the sun hour S_h =4.69 h obtained from our previous research conducted in Malaysia [39]. Then, the number of PV panels is calculated from Eq. 8- the power ratio of watt-peak and manufactured rated PV.

In Table 1, the PV sizing is calculated based on the load power and its daily usage. If the number of *autonomous day* is 1 and daily usage is 2 h, the required energy is found to be 780 Wh/day, which yields a minimum size of 166 W PV panel.

TABLE 1. Calculation of PV sizing based on Eqs. 5 - 8.

Parameters of Eqs. 5,6,7,8						$P_{pv,peak}$ (W) Eq. 7	P_{max} (W)	N_{pv} Eq. 8
P_{load} (W)	h_{load} (h/day)	E_{load} (W-h) Eq. 5	Energy loss (30%)	E_{pv} Wh/day Eq. 6	S_h (h)			
300	2	600	1.3	780	4.69	166.31	425	0.39≈1

The obtained capacity of 166 W_p represents the Watt-peak of the solar PV, achievable only under STC – with 1000 W/m^2 solar irradiance and an ambient temperature of 25 ^oC. To account for varying conditions, we have opted for a larger Monocrystalline PV panel with a capacity of 425 W_p. This decision is rooted in our prior empirical research conducted in Malaysia, where we observed an average solar irradiance of 512.37 W/m^2 and an average ambient temperature of 33 ^oC. The environmental factors, as highlighted in [39], notably impact PV output performance. The panel is strategically installed at a 23-degree tilt angle at the project site, and its detailed specifications can be found in Table 2.

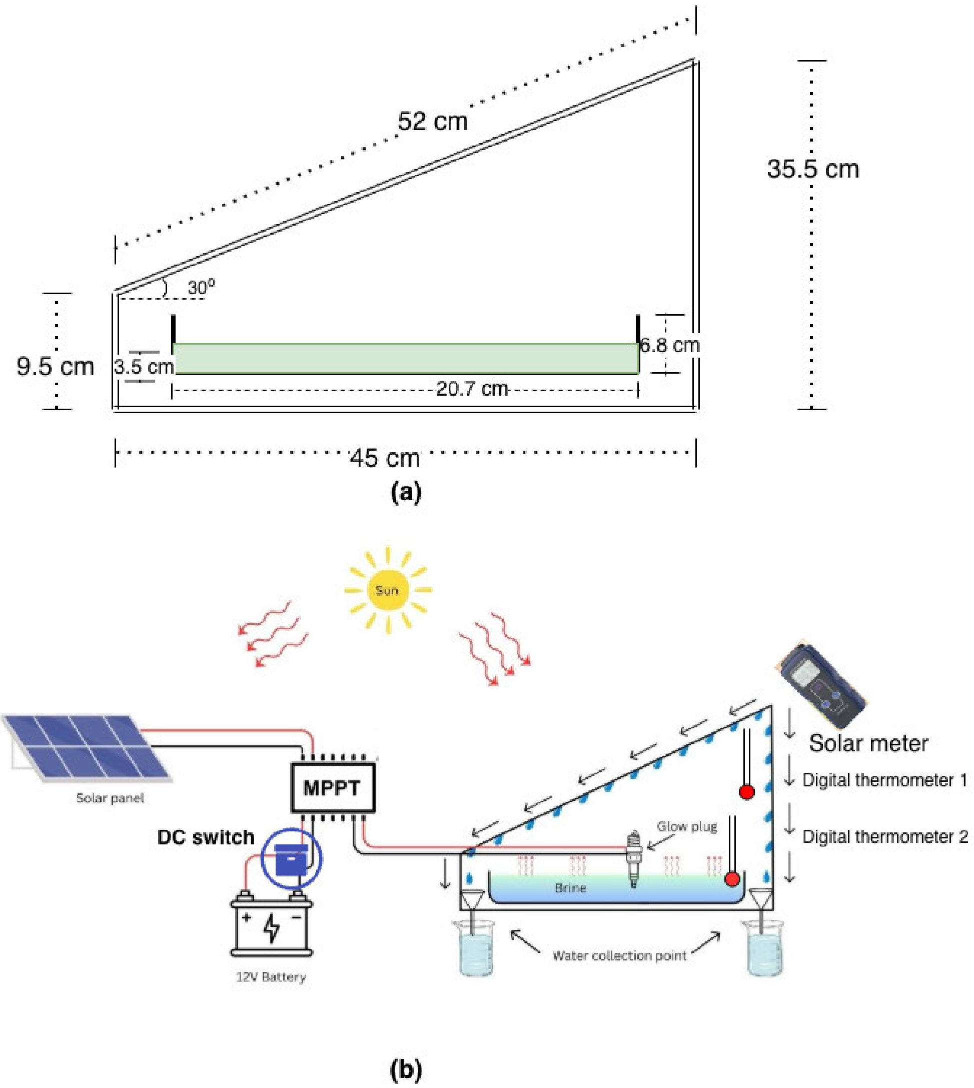

FIGURE 4. Physical and electrical design of solar still. (a) Dimension of single solar still; (b) Electrical circuit diagram of glow plug and its connectivity with PV powered battery. Hexagon nuts, flange, cramp terminals are used for solid connection. The polarity of 95 mm glow plug is separated by an insulated black ring. Aluminum composite holder positioned the glow plug above the brine water container, ensuring the heating element is fully submerged. Digital thermometers and solar meter measure brine and chamber temperatures and irradiance, respectively.

TABLE 2. Specification of Monocrystalline PV – manufacturer provided datasheet at STC.

Parameters	Values
Maximum power, P_{max}	425 W
Open circuit voltage, V_{oc}	49.09 V
Voltage at MPP, V_{mpp}	41.39 V
Current at MPP, I_{mpp}	10.27 A
Short circuit current, I_{sc}	10.78 A
Module efficiency	19.7%
Weight	24.5 / 54 [kg / lbs]
Manufacturer	QCells
Maximum system voltage	DC 1500 V

E. BATTERY SIZING

The sizing calculation of battery is important and needs to be done correctly to provide rated power to the load without any failure. The calculation was made by using formula shown in Eq. 9.

$$CB = \frac{E_{load}}{B_{loss} \times B_{DoD} \times V_{nom}} \times autonomous\ day \qquad (9)$$

Here, CB and V_{nom} refer to the battery capacity (Ah) and nominal voltage of the battery (V), respectively. B_{loss} and B_{DoD} denote battery loss and battery depth of discharge and usually constant value of 0.85 and 0.70, respectively are used for a deep cycle lead acid battery. Considering $autonomous\ day = 1$ and $V_{nom} = 12$ V, minimum 84.0 Ah capacity of battery should be used for the SPWH system. A lead acid battery of 12 V 100 Ah capacity is considered in this study.

F. MPPT SELECTION

To select the appropriate size of the MPPT charge controller, we have determined the rated open circuit voltage and maximum charge current. The mathematical models shown in Eq. 10 and Eq. 11 determine these two parameters. First, Eq. 10 obtains the rated open circuit voltage ($V_{oc,r}$) from the open circuit voltage of the panel (V_{oc}), number of panels connected in series ($N_{pv,series}$), and temperature correction factor (T_{factor}).

$$V_{oc,r} = V_{oc} \times N_{pv,series} \times T_{factor} \tag{10}$$

Refer to Table 2, we can obtain $V_{oc} = 49.09$ V, $N_{pv,series} = 1$ (one PV module), and $T_{factor} = 1.2$ (based on ambient temperature 33 °C in Malaysia). This yield rated open circuit voltage, $V_{oc,r} = 58.90$ V.

Eq. 11 has determined the maximum charge current, (I_{mc}) by the ratio of total required power ($P_{max} \times N_{pv}$) and battery charge voltage (V_{bc}). Based on the battery specification, $V_{bc} = 14.7$ V for a 12 V battery, which yields $I_{mc} = 28.91$ A for this research. Therefore, we have purchased an MPPT solar charge controller with a specification of 75 V 50 A.

$$I_{mc} = \frac{P_{max} \times N_{pv}}{V_{bc}} \tag{11}$$

The sizing calculation determines the minimum required capacities of the solar PV and the battery for reliable system operation. Oversizing the PV panel enables faster battery charging and improves energy availability, particularly under low irradiance conditions. At low brine temperatures, the heating element draws a high current, which increases the battery discharge rate and effectively reduces the available battery capacity due to Peukert effects and voltage sag. By employing an oversized PV (from 166 W_p upsizes to 425 W_p), higher charging currents can be achieved, allowing the battery to recover more rapidly even during periods of moderate solar irradiance. During operation, the battery voltage and current are regulated by the MPPT charge controller, which mitigates excessive voltage drop and maintains stable system performance. The upsized 425 Wp PV panel has a rated maximum power point voltage (V_{mpp}) of 41.39 V, and the MPPT controller converts this excess voltage into higher current for fast charging of the battery. This replenishes the 100 Ah battery faster when intermittent high-discharge events occur due to the 300 W (25 A) glow plug load.

G. SYSTEM EFFICIENCY

The efficiency of the proposed system can be determined from the thermal characteristics of the systems according to the principles of the first law of thermodynamics. The efficiency of the SPWH with a glow plug is defined as the ratio of the daily output energy for distilled freshwater to the input energy from solar radiation during the experimental period. The system efficiency (η) of the proposed system is determined using Eq. 12 [45], [46].

$$\eta = \frac{M_{cum} \times S_l}{A \times Z \times t} \tag{12}$$

where M_{cum} = amount of total freshwater productivity in kg, A =area of solar still in m^2, Z = average solar irradiance in W/m^2, and t = total experimental time in seconds (s).

It is important to note that the latent heat of evaporation of water, denoted as S_l in J/kg, can be computed using the formula provided in Eq. 13 or Eq. 14.

When temperature, $T > 70$ °C,

$$S_l = 3.16 \times (10^6 - 761.6 \times T) \tag{13}$$

If $T < 70$ °C, alternative Eq. 14 can be considered.

$$S_l = 2.49 \times (10^6 - 947.79 \times T + 0.131 \times T^2 - 0.005 \times T^3) \tag{14}$$

where, $T = \frac{T_{still}+T_{brine}}{2}$.

H. PHYSICAL DESIGN OF SINGLE SOLAR STILL

Single solar still chamber is developed to execute the desalination process and freshwater collection from brine water. This design is perfect for desalination in isolated or resource-constrained locations. Although single solar still produces less water than more sophisticated designs, it is simple to build and maintain for the rural inhabitants. In this study, we adopted a simplified approach to the physical design of a single solar still, taking into consideration of the remote island conditions where local inhabitants can easily fabricate the system. The physical design of the still can be found in our previous studies, e.g. [47], and others [4], [22]. However, like [47], we did not consider PVC pipe system and separated condenser for simplicity of the design. This decision aligns with the main objective of the study to analyze the performance of glow plug heater during early hours or low irradiance conditions, where rapid heating of brine water is crucial to initiate evaporation alongside passive solar heating.

Like our previous implementation of [47], the structure of the active solar still is built on PVC pipe, which was engulfed with super clear PVC transparent sheet. These materials are cost effective, easy to fabricate for rural people, non-corrosive and high durability, and lightweight. The glow plug heating element is integrated inside the single solar still, submerged in the brine. The main components of the solar still are (shown in Fig. 4): PVC pipe structure, super clear PVC sheets, Aluminum composite with glow plug, and tray with brine water. Aluminum container was placed around the solar still to collect the condensed freshwater. In this design, both evaporation and condensation process are occurred in the same section of the still. The evaporator section was covered with super clear PVC sheet, so that brine temperature heated by sunlight and glow plug is retained within the evaporation section. The hole in the PVC pipe allowed airflow circulation and enhanced the condensation process. Besides this, the system was installed in an open space, therefore sufficient natural wind flow passed over and surrounding the chamber. This naturally enhanced the condensation process. We did not install any water pump to supply brine into the basin. Because residual salt is needed to be cleaned frequently after brine evaporation. Based on our experience, the salt accumulation reduces the evaporation rate and disturb the heating element of the glow plug. This leads to malfunction of the overall system. Adding a water pump increases the design complexity and require extra energy for the system.

Fig. 4(a) shows the dimension of the single solar still covered by clear PVC transparent sheet, polyvinyl chloride aka PVC material with a thickness of it 0.15 mm. The sheet possesses clear thickness with very low toxic additives. This also minimizes the risk of toxic contamination in the produced freshwater water. The dimension of the solar still chamber is 35.5 cm × 22 cm and the total size of the pipe used is approximately 372 cm.

Using the circuit diagram, the experimental setup is constructed, shown in Fig. 5. The brine water is held in the Aluminium container-1, size 20.7 $cm \times 20.7$ cm (or 0.043 m^2) of length and width placed under the still chamber. The foil container provides high heat capability from the sun and maintains hygienic. Black painted coating can enhance the absorb capability of heat, however it was avoided due to risk of chemical contamination with freshwater. The roof of the chamber is designed in an inclined shape and allows sunlight entry for internal heat buildup. This design facilitates efficient condensation of vapor on the inner plastic surface of the roof. Aluminium Container-1 serves as the evaporation tray. Aluminium is selected due to its high thermal conductivity, which supports rapid heat transfer from the glow plug to the brine. Aluminium Container-2 is placed outside the chamber and used as the collection basin for the condensed freshwater. The inclined roof directs the condensed water toward an outlet, ensuring clean and efficient water collection. To hold the glow plug over the Container-1, an aluminium composite sheet is used, which ensures that the apex of the plug is not touched by the container plate. The composite sheet is stiff and has very high resistance with non-oxidation characteristics, which makes it suitable for holding the glow plug. The length, width, and thickness of it are 0.3, 0.05, and 0.005 m respectively.

I. INSTALLATION SETUP

The experiment was conducted at the solar site located at coordinates 1.8653778 latitude and 103.0894774 longitude, within the Faculty of Electrical and Electronic Engineering at the Universiti Tun Hussein Onn Malaysia (UTHM), Johor, Malaysia. Brine water samples were collected from Senggarang, Johor, Malaysia. To gather data, various electrical parameters including battery voltage, battery current, PV current, and PV voltage are meticulously recorded via the MPPT controller. Additionally, an environmental data collection system featuring a solar irradiance meter and a temperature data logger was employed. The digital thermometer recorded temperature variations at five-minute intervals during the heating process for brine, chamber, and ambient temperatures. A SM206 Digital Solar Power Meter was used to record irradiance data at the same interval. No thermohygrometer was used to measure humidity in this study as previous studies, such as [32] and [48] have indicated that the most dominant environmental factors for evaporation are radiation intensity and ambient air temperature. Finally, the harvested freshwater was quantified using a digital scale. The freshwater quality was evaluated using a self-developed water quality monitoring system consisting of a pH sensor, a turbidity sensor, and a total dissolved solids (TDS) sensor. The pH, turbidity, and TDS sensors measure the acidity or alkalinity, the cloudiness associated with suspended particles, and the concentration of dissolved ions and other solids (e.g., salts) in the freshwater, respectively.

Fig. 6 illustrates the installation setup and the freshwater production process from brine. At the start of the experiment, the brine water level in Aluminium Container-1 was initially set at 3.5 cm, an optimal depth based on our previous study [48]. The solar still chamber condenses water vapor into liquid, which is subsequently collected and stored in Aluminium Container-2.

At the core of the energy management system, the MPPT controller assumes a central role. With this controller in place, the solar PV system maximizes its power output to efficiently charge the battery. Subsequently, it enables the battery to deliver power to the DC load, specifically the glow plug. The connection between the MPPT controller and the glow plug is facilitated through the designated load connection. Similarly, the PV array and the battery establish their seamless integration into the system via dedicated connections to the MPPT controller.

The 300 W glow plug, 12 V DC configuration falls within the Safety extra-low voltage or SELV category. It is operated from a solar PV–battery system that is electrically isolated from the grid. Referring to the standard IEC 61140 and IEC 60364-4-41, this 12 V DC system is deemed safe for human contact because the source is galvanically isolated and operates as a floating system without an earth reference. This significantly reduces the risk of electric shock compared to grid-connected or high-voltage systems. To mitigate water ingress and corrosion in the brine environment, the feedthrough of the glow plug is required to be cleaned manually whenever there is a accumulation of corrosion. The heater current is inherently controlled by the MPPT charge controller, thereby reducing fault energy. Conventional AC ground-fault protection devices (e.g. RCD/GFCI) are not applicable to this isolated extra low-voltage DC system. Therefore, the formal insulation resistance testing and ground-fault monitoring were not implemented in the study. As an additional safety measure, a DC switch was installed between the battery and the MPPT controller for safe system ON/OFF operation, avoid sparking during switching and abnormal operation.

III. RESULT ANALYSIS

A. ANALYSIS ON BATTERY CAPACITY

Using Eq. 9, the size of battery capacity (*CB*) has been analyzed against daily load hour (h_{load}) and *autonomous day*. Fig. 7 shows that *CB* increases linearly with both parameters. However, a significant finding from the analysis is that an increase in the number of autonomous days can lead to a higher *CB*. This means that, when considering *CB*, achieving longer h_{load} per day is comparatively more cost-effective than increasing the number of autonomous days. For example, powering the 300 W glow plug for 5 hours with an $autonomous\ day = 1$ is almost 9 times cheaper than battery capacity compared to powering it for 1 day with an $autonomous\ day = 5$.

B. ENVIRONMENTAL AND ELECTRICAL PARAMETERS' ANALYSIS

The experiment was carried out over a two-hour period, from 12:00 to 2:00 PM. Electrical data from the PV, battery, and environmental parameters were collected every 5 minutes during this time. Fig. 8 shows environmental parameters, such as solar irradiance and ambient temperature that was recorded during the experimental day. As stated earlier, the ambient temperature does not fluctuate throughout the year under the climate of Malaysia due its position near the equator. The average temperature was recorded 33.96 ^{o}C, whereas the standard deviation is calculated as 0.53. This indicates that temperature is less dispersed from the average value. In contrast, the average solar irradiance was recorded 418.56 W/m^2, where the standard deviation is 76.84 – relatively high from the mean value. This is because, cloud covered in this region is between 6 and 8 which is a significant phenomenon that impacts solar energy generation, shown in Fig. 8. It plays a major role in modulating the amount of solar irradiance – for instance, increase from 376 to 531 W/m^2 in 15 minutes between 12.30 and 12.45 PM. This impact has been mitigated through appropriate design of battery sizing integrated with PV for effectively handling the fluctuating shifts in solar power extraction.

Fig. 9 shows results of PV current against solar irradiance. It shows the relationship between these two parameters is found to be logarithmic. The degree of relationship is moderate as the value of R^2 =0.407. From the positive correlation confirms that solar irradiance is a key driver of output current. However, the relationship indicates a steep rise in current at low irradiance, while at higher irradiance, the growth tapers off. This trend is consistent with typical PV behavior under non-linear operating conditions, influenced by factors such as the negative temperature coefficient of monocrystalline PV modules and intermittent cloud cover. In addition, the R^2 indicates that 40.7% of the variation in PV output current can be attributed to changes in irradiance. The remaining 59.3% is influenced by other environmental factors, such as module temperature and cloud cover.

Fig. 10 illustrates a comparison between battery current and PV current. It is evident that the battery current exceeds the PV current due to the high current consumption of the glow plug load. This consumption causes the battery to discharge rapidly before it is recharged by the PV source. Notably, at 13:50, when the PV current began to rise (reaching 5 A), the battery also delivered more current to the load (reaching 21.2 A). During the observation period, the battery current varies between approximately 12.9 A and 21.2 A, indicating fluctuations in the charging rate. The current reaches its first peak of about 21 A at around 12:40, which corresponds to solar irradiance exceeding 500 W/m^2, enabling a higher charging to the battery. After this peak, the battery current gradually decreases to around 13–14 A between 13:25 and 13:40, which can be attributed to a temporary reduction in solar irradiance. A second peak of approximately 21.2 A occurs at around 13:50. Although the irradiance level remains moderate during this period, the increase in current indicates the load demand have contributed to higher power flow through the battery. Despite fluctuations in both solar irradiance and battery current, the system consistently ensures power supply to the load without interruption.

Fig. 11 demonstrates minimal voltage fluctuations in both output of PV array and load (battery) as they supply power to the glow plug during the entire experiment. The PV voltage and battery voltage shown in Fig. 11 correspond to the voltages measured at the output terminal of the MPPT controller. The system utilized an MPPT charge controller to ensure that the glow plug load receive a regulated output voltage while allowing the current to vary according to the available solar irradiance. Since PV output fluctuates with irradiance, the MPPT controller continuously adjusts its operating point to maintain the output voltage at its terminal while tracking the maximum power point. The controller also prevents the battery from being fully discharged or overcharged. From Fig. 11, an initial voltage-shift of 0.9% is observed, attributed to the switching effect. The consistent behavior of the selected MPPT charge controller in maintaining voltage regulation within 5% efficiency is evident from the overall findings. In practical electrical systems, voltage variation within approximately ±5% is considered acceptable for stable operation of connected loads, as indicated in electrical power standards such as IEC 60038 and PV system monitoring guidelines in IEC 61724 − 1. In this study, the measured PV and battery voltage variation was less than 0.9%, indicating stable operation of the power supply during the experiment.

The variation of PV and battery power during the daytime operation is presented in Fig. 12. At the beginning of the observation period, the battery power is approximately 179.85 W, which gradually increases as the PV generation improves. Between 12:05 and 12:30, the battery power remains relatively stable in the range of 192–198 W,

FIGURE 5. Fabrication of solar still chamber with the glow plug heating system. The chamber is PVC pipe structured enclosed with transparent plastic cover. Solar radiation enters through the cover and heating the brine water in Aluminium Container-1. The vapor condenses on the inner surface of the cover and is collected as freshwater in Aluminium Container-2.

indicating a steady charging condition where the PV output sufficiently supplies the battery and system demand. A significant increase is observed at approximately 12:40, where the battery power reaches 226.8 W, indicating a temporary improvement in solar irradiance that enhances the charging capability of the PV system. Following this peak, the battery power gradually decreases to about 172.8 W at around 12:50, and subsequently stabilizes near 183 W for a short period. The reduction in power can be associated with fluctuations in solar irradiance or partial variations in the glow plug load. After 13:10, the battery power continues to decline, reaching a minimum value of approximately 139.32 W around 13:40, which indicates reduced available PV power during that interval. A second power surge occurs at approximately 13:50, where the battery power increases sharply to 228.96 W. This increase demonstrates the system's capability to capture and store additional solar energy when irradiance conditions improve. After this peak, the battery power returns to a stable level of around 194 W toward the end of the observation period.

Overall, the figure demonstrates that battery charging power follows the variation of PV output, highlighting the dependence of the storage system on instantaneous solar availability. The total electrical energy delivered by the battery to the glow plug during the observation period was calculated by integrating the measured battery power over time. Considering a sampling interval of 5 minutes (0.083 h), the accumulated electrical power and energy supplied to the load was approximately 4527.93 W and 377.3 Wh (0.377 kWh), respectively.

C. FRESHWATER PRODUCTION AND ENVIRONMENTAL PARAMETERS ANALYSIS

Based on our observations and findings from previous studies, the freshwater production is significantly dominated by solar irradiance that increases both brine and chamber temperatures. As previously highlighted, the production rate increased with rising solar radiation and decreased as the radiation intensity declined. Fig. 13 shows the correlation coefficient between amount of freshwater in every 5 min against the brine temperature. The relationship shows that amount of freshwater is proportional to brine temperature when the ambient temperature is considerably constant. The regression model obtained from this experimental data can be shown in Eq. 15.

$$M_{cum} = 0.0455 \times T_b - 1.9266 \tag{15}$$

Here, M_{cum} and T_b refer to the amount of freshwater production and brine temperature respectively. From the derivatives of the Eq. 15, it can be explained that approximately 0.0455 gm of freshwater can be produced at every 1 ^{o}C increase in brine temperature.

We also observed that the hourly freshwater yield of the solar still shows a similar pattern with that of previous studies, such as [47] to the variation in solar radiation intensity. Moreover, the linear equation of previous study confirms the 0.0457 g/^{o}C freshwater production, which also support the outcome of this experiment. This behavior is linear (R^2 = 0.905) with trends reported in previous studies.

Fig. 14 illustrates the temporal variation of freshwater yield together with brine, chamber, and ambient temperatures between 12:00 and 14:00. The presented data show the amount of freshwater produced at every 15th minute. The results indicate a strong thermal dependence of freshwater production on brine temperature, which was controlled by the glow plug enabled SPWH system. The production of freshwater is increased from 0.78 g at 12:15 to a maximum of 1.68 g at 12:45. This increase corresponds to the rise in brine temperature from approximately 62 to 78 ^{o}C. Since the ambient temperature was recorded between 33-35 ^{o}C,

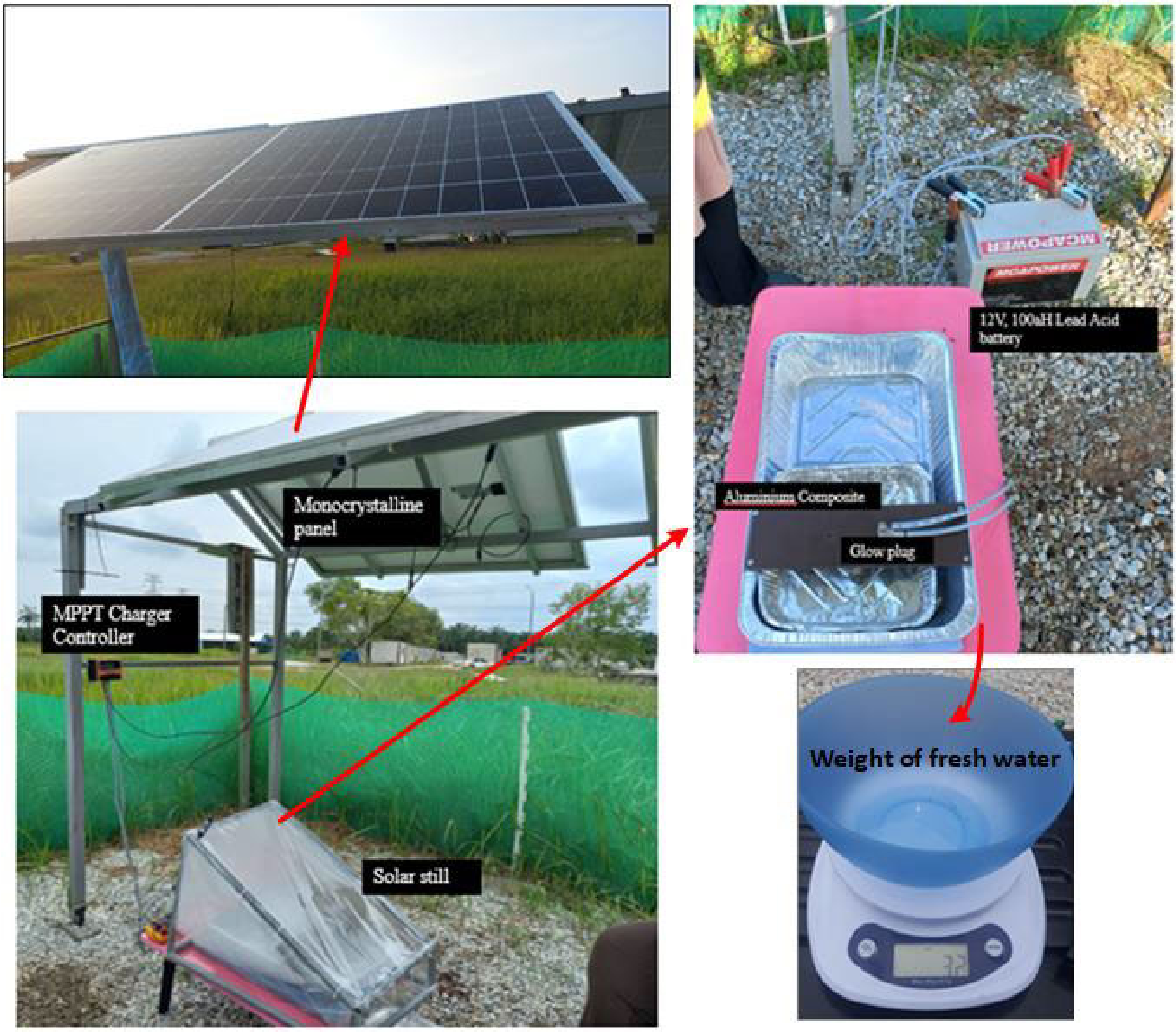

FIGURE 6. Installation setup for harvesting freshwater from brine water, solar site, FKEE, UTHM. Electrical design consists of mono type solar PV, MPPT charge controller, safety switch, and battery.

the results confirm that evaporation was mainly driven by the external catalyst SPWH system, which converts sunlight into thermal energy. The result also shows that the freshwater production was nearly same at 15 min-intervals, within the range of 1.68 to 1.48 g between 12:45 and 13:45. This confirms that SPWH system can maintain a steady freshwater production when both ambient temperature and irradiance are low.

Fig. 15 presents the variation of freshwater production represented by bar columns (g per 15 min) against the solar irradiance as a line plot (W/m^2). Solar irradiance shows a generally decreasing trend from 12:00 to 13:30, dropping from approximately 600 W/m^2 to a minimum of 320 W/m^2. This fluctuation reflects typical short-term variations in solar irradiance influenced by cloudy conditions. In contrast, freshwater production increases steadily after the start of operation, reaching a maximum between 12:45 and 13:15. It is observed that the peak freshwater production does not coincide with the maximum irradiance due to the presence of the SPWH system. Consequently, steady water production was maintained even as irradiance declines, indicating that freshwater generation was primarily controlled by the SPWH system. In this technique, the primary role of the solar irradiance was to charge the battery through solar PV, which powering the system. Here, both irradiance and ambient temperature act as secondary contributors for maintaining the brine temperature to ensure that the freshwater production is independent of the climatic conditions. This outcome shows that the SPWH system can be very effective during winter season when ambient temperature is low with moderate level of solar irradiance. Moreover, crystalline silicon–based solar PV performs more efficiently at lower ambient temperatures. This technique differs from the previous studies, where experiments were conducted under the summer hot conditions and freshwater production was primarily dependent on both solar irradiance and ambient temperature.

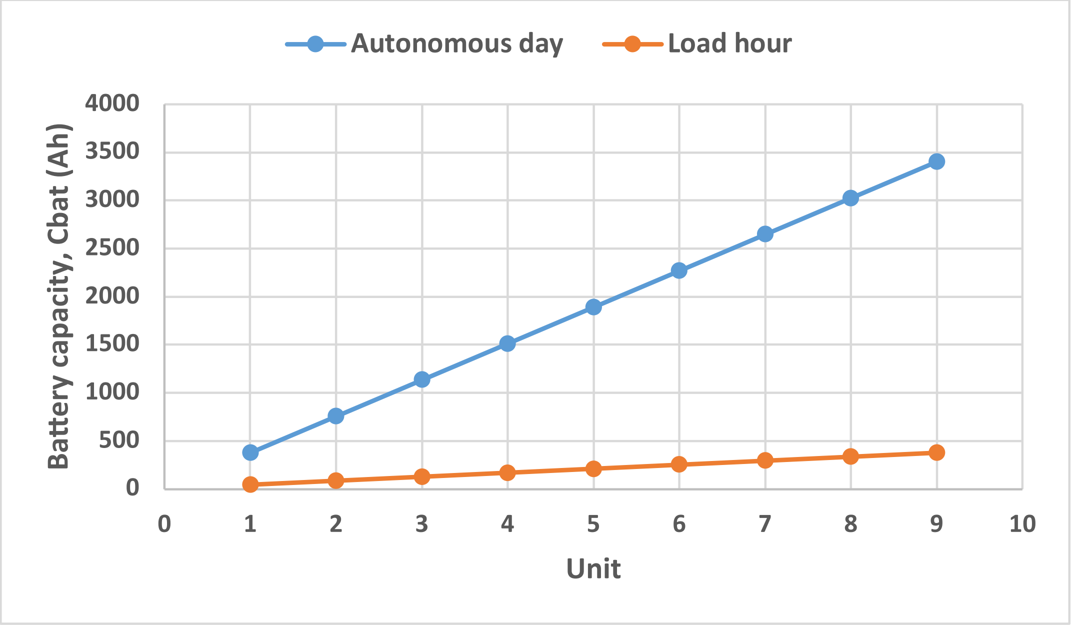

FIGURE 7. Analysis on sizing of battery capacity (*CB*) against load hour (h_{load}) and number of autonomous day at P_{load} = 300 W. Blue line indicates *CB* against autonomous day when h_{load} = 9 h. Orange line refers *CB* against load hour (h_{load}) when *autonomous day* = 1.

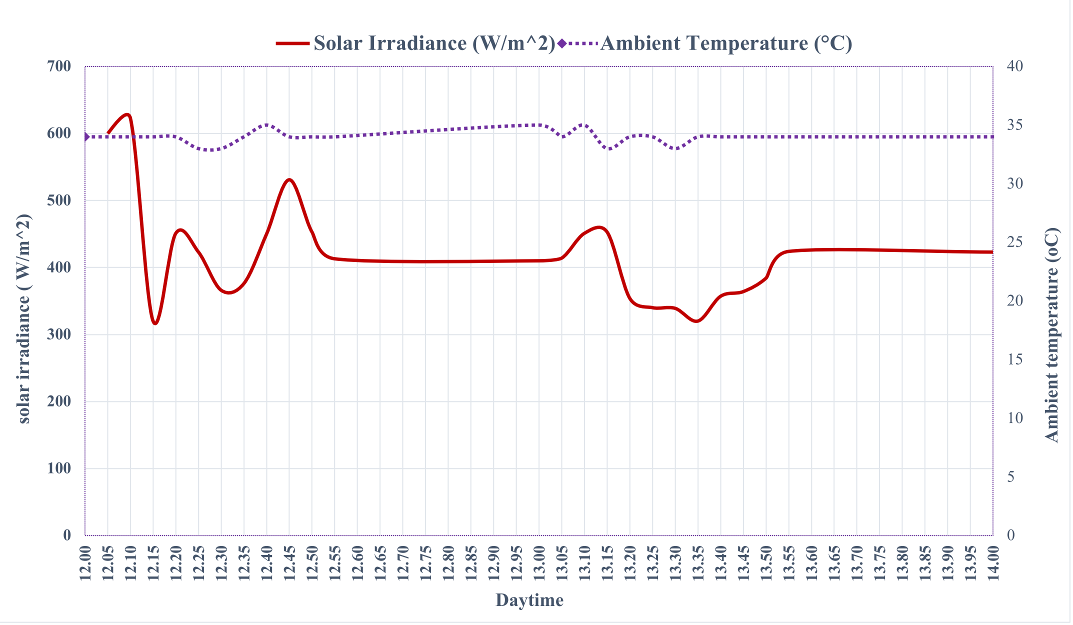

FIGURE 8. Solar irradiance and ambient temperature on the experimental day. The fluctuation of solar irradiance indicates high cloud cover in Malaysia.

D. ANALYSIS ON SYSTEM PERFORMANCE

Upon completion of the experiment, a total of 0.032 kg of freshwater was generated from an initial 4.5 kg of brine water. Table 3 presents the comprehensive range of environmental parameters and temperatures, encompassing maximum, minimum, and average values for both the brine water and the solar still chamber. This outcome translates corresponds to 0.032 kg of freshwater from an area of 0.043 m^2 over a span of 2 hours. Extrapolating this process to a daily operation of 9 hours, assuming solar irradiance exceeds 400 W/m^2, the proposed system exhibits the potential to yield a remarkable daily freshwater production rate of 3.35 kg/m^2.

The extrapolated freshwater production pf 3.35 kg/m^2 per day was assumed from the 9 hours experiment with an average measured solar irradiance of 418.56 W/m^2 (Min 320 and

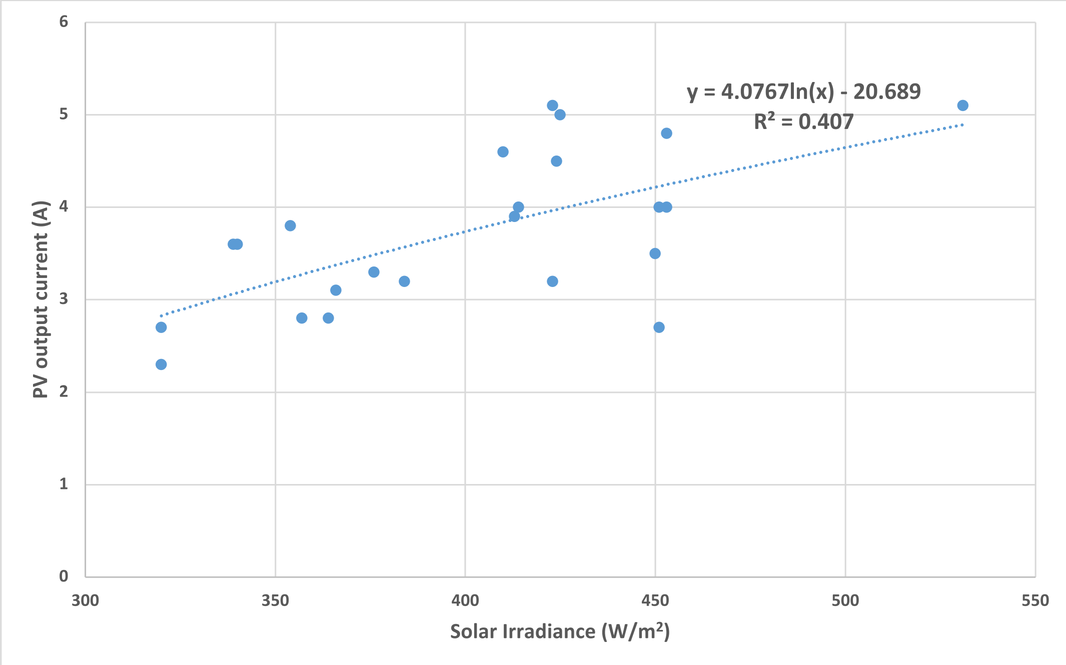

FIGURE 9. PV output current against solar irradiance- logarithmic moderate relationship due to negative temperature coefficient of the monocrystalline PV module.

TABLE 3. Maximum, minimum, and average data of environmental parameters, brine and solar still chamber.

Parameters and unit	Symbol	Maximum	Minimum	Average
PV voltage (V)		11.9	11.8	11.9
PV current (A)		5.1	2.2	3.6
Battery voltage (V)		10.9	10.8	10.8
Battery current (A)		21.2	12.9	16.8
Solar irradiance (W/m^2)	Z	623	320	418.6
Ambient temp (^{o}C)	T_{amb}	35	33	33.96
Brine water temp (^{o}C)	T_{brine}	79.2	36	70.58
Solar still chamber (^{o}C)	T_{still}	60	34.8	49.2
System efficiency (%)	η	49.83 (1st hour) and 68.18 (2nd hour)		

TABLE 4. Comparison between theoretical and experimental data of brine water.

Theoretical			Experiment		
Initial Temp (^{o}C)	Final Temp (^{o}C)	Time (min)	Initial Temp (^{o}C)	Final Temp (^{o}C)	Time (min)
35	80	46.72	36	79.2	45

Max 623 W/m^2) and an ambient temperature of 33.8 ^{o}C. This assumption is justifiable because this was the average irradiance recorded on the experimental day in Malaysia. Accordingly, the reported 3.35 kg/m^2 per day should be interpreted as a lower-bound estimate of daily freshwater production under low-irradiance or cloudy conditions, rather than as a precise full-day yield. The extrapolated yield is also consistent with previous experimental studies conducted in Malaysia using a similar design of active solar still with PVC hot water, which reported productions of 2.21 kg/m^2 per day amount of freshwater [47] On the other hand, freshwater yields of 1.55 and 1.69 kg/m^2 per day were reported for a solar still without any heating element [48] and for a passive solar still [47], respectively.

The thermal efficiency is determined to assess the operational effectiveness of the glow plug enabled SPWH under the available environmental conditions. The system efficiency was calculated for the first and second hours of the experiment using Eq. 12. Since $T = \frac{T_{still}+T_{brine}}{2} < 70$ ^{o}C for both cases, the latent heat of evaporation, S_l was calculated as 2353096.05 and 2347743.38 Jkg^{-1} respectively, using Eq. 14. During the first hour, the recorded average T_{still} and T_{brine} were 67.3 and 50.4 ^{o}C, respectively and while the second hour they were 74.13 and 47.95, ^{o}C respectively. The average freshwater productions during the first and second hours were 0.0147 kg and 0.01736 kg, and the corresponding average solar irradiance values were 448.46 and 386.17 W/m^2, respectively. Using Eq. 12, the calculated hourly efficiencies were 49.83 and 68.18%, yielding an average efficiency of approximately 59%. The calculation method was adopted from [45] and [46], and the obtained results are consistent with those previous studies, which reported efficiencies of 52.5 and 63.5%, respectively. The efficiency results are shown in Table 3.

Fig. 16 shows the temperature difference between brine water and solar still chamber. The highest temperature of the brine water reached 79.2 ^{o}C at 12:45 PM, within 45 min of the experiment. At the same time, the temperature of water vapor is found to be 60 ^{o}C. The temperature has started to decrease because the current from the battery is not sufficient. This happens due to the decrease in solar irradiance on the experiment day.

Table 4 shows the time taken to increase temperature for 4.5 kg of brine from 35 to 80 °C. The theoretical time taken is derived from the model equation, which neglect heat losses and auxiliary solar gains. In the experiment, heat losses due to convection, evaporation, and conduction act to increase the heating time, while solar irradiance transmitted through the transparent cover provides an additional heat input that reduces the heating duration. As a result, these opposing effects partially compensate for each other. The observed difference between the calculated (46.72 min) and measured (45 min) heating times is therefore attributed to this partial compensation, rather than very precise value.

Fig. 17 shows the progressive temperature escalation, spanning from the initial temperature of 36 °C to the peak of 79.2 °C, at five-minute intervals. This rise demonstrates a clear linear trend, exhibiting a strong regression relationship with time. Both mathematical models have been adeptly fitted to the data points, yielding a $R^2 = 0.87$. The chamber temperature is inherently transient because evaporation and condensation occur simultaneously during operation. In this study, linear fits are applied the 2-hour experimental period, during which both brine and chamber temperatures shows a near-linear trend. Similar to this study, the non-linear temperature profiles were also observed by a recent study in [32]. The non-linear curve is represented by a second-order polynomial fit for both temperature profiles, with an $R^2 = 0.98$. A detailed transient energy balance incorporating convective, conductive, and vaporization losses is not included in the work and will be addressed in future studies.

The linear regression equations for the brine water and solar still chamber can be derived as Eq. 16 and Eq. 17, respectively.

$$T_{brine} = 0.955 \times t + 43.042 \tag{16}$$
$$T_{still} = 0.6176 \times t + 37.095 \tag{17}$$

where, T_{brine}, T_{still}, and t denote temperature for brine (°C), solar still (°C), and time (min) respectively. The observed slope signifies a positive correlation between temperature and time. Furthermore, upon deriving the derivatives of both equations, Eq. 18 and Eq. 19 can be obtained.

$$\frac{d(T_{brine})}{dt} = 0.955 \tag{18}$$
$$\frac{d(T_{still})}{dt} = 0.6176 \tag{19}$$

Both equations describe the rates of temperature increase. This can be interpreted by considering that, at every one-minute interval, the temperature of the brine water increases by 0.96 °C, while the temperature of the solar still chamber increases by 0.62 °C (up to a saturation point).

The above analysis indicates that brine water heats up faster than the chamber temperature due to better thermal absorption and active heating by glow plug. The brine water also remains relatively stable, with minimal fluctuations of ± 2 °C, which supports sustained freshwater production. In contrast, the chamber temperature shows more variability due to loss of ventilation and the influence of the surrounding air condition. The temperature difference between brine and chamber increases slightly over time (22-28 °C), indicating that brine retains heat better than the chamber. This happens because water has a higher specific heat and some heat may be released from the chamber through convection during the experimental time.

In Fig. 18, we analyzed the required time from 35 to 80 °C against the amount of brine. The required time was estimated using the analytical model stated in Eq. 3. The results show a nearly linear relationship between brine mass and heating time. As the brine quantity increases from 3 kg to 8 kg, the required heating time increases proportionally from approximately 31 min to 83 min. This trend is expected because the thermal energy required to raise the temperature of the brine is directly proportional to its mass. It also indicates that the temperature of the 4.5 kg brine can be reached to 80 °C in 46.72 min, whereas the experimental time is found to be 45 min. The analytical model in Eq. 3 estimates the heating time using the energy balance, which assumes ideal conditions without explicitly accounting for thermal losses. The primary purpose of this formulation was to provide a first-order estimation of the heating requirement for different amount of brine. In the experimental setup, the heater was directly immersed in the brine, which enabled efficient heat transfer with minimal thermal resistance. In addition, the transparent plastic cover allowed partial solar heat gain, which contributed additional thermal energy to the brine. These factors partially compensated for the unaccounted thermal losses (such as convection and radiation to the surroundings), resulting in the close match between the theoretical heating time (46.72 min) and the measured time (45 min) for 4.5 kg of brine.

Fig. 19 illustrates the correlation between brine water and solar still temperatures with solar irradiance over the course of the day. In the initial phase of the experiment, spanning from 12:05 to 12:30 PM, a decline in irradiance was observed due to an approximate cloud cover of 7. During this period, both the brine water and chamber temperatures showed an upward trend, attributed to the heating effect of the glow plug. This deliberate heating helped increase the evaporation rate over time. Notably, during the two-hour experiment, the brine temperature remained stable despite fluctuations in solar irradiance. This consistent behavior of brine temperature is observed as a significant and noteworthy outcome of this research.

E. ELECTRICAL AND THERMAL ENERGY BALANCE ANALYSIS

The electrical energy supplied to the glow plug heater was estimated by integrating the measured output power over the experimental period (12:00–14:00). This results in an input of total electrical energy ($E_{electrical}$) is approximately 377.3375 Wh or 1.36 MJ (Fig. 12). This electrical energy contributes primarily to heating the brine water and partially

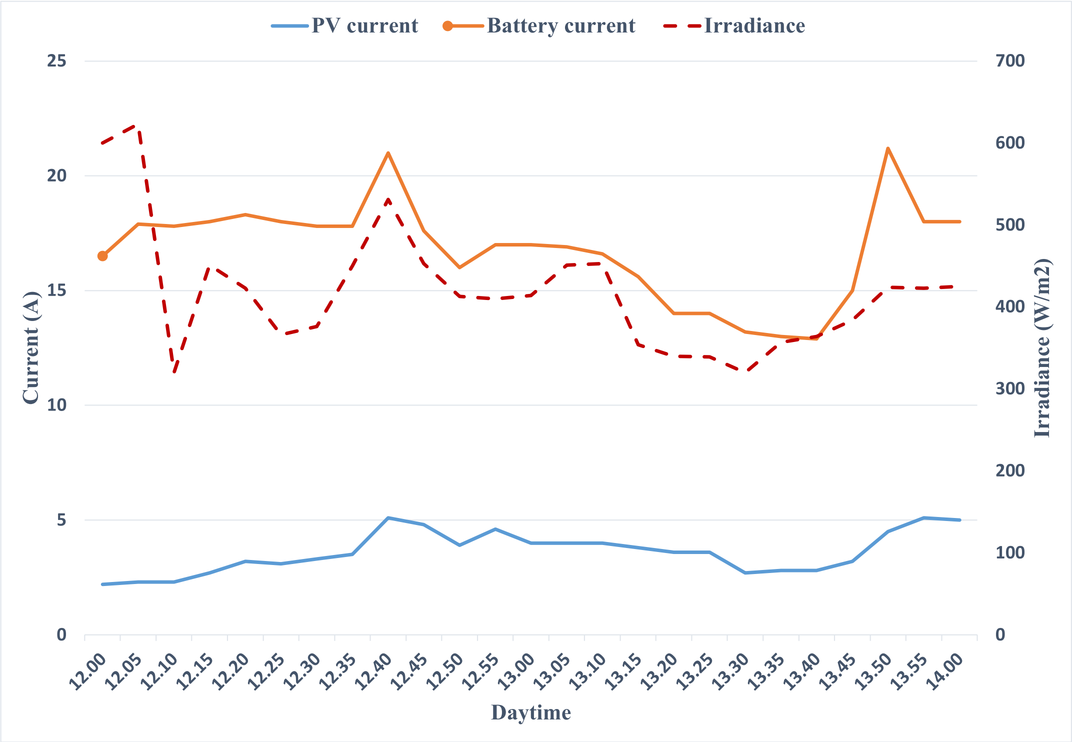

FIGURE 10. Irradiance, PV, and battery current against daytime.

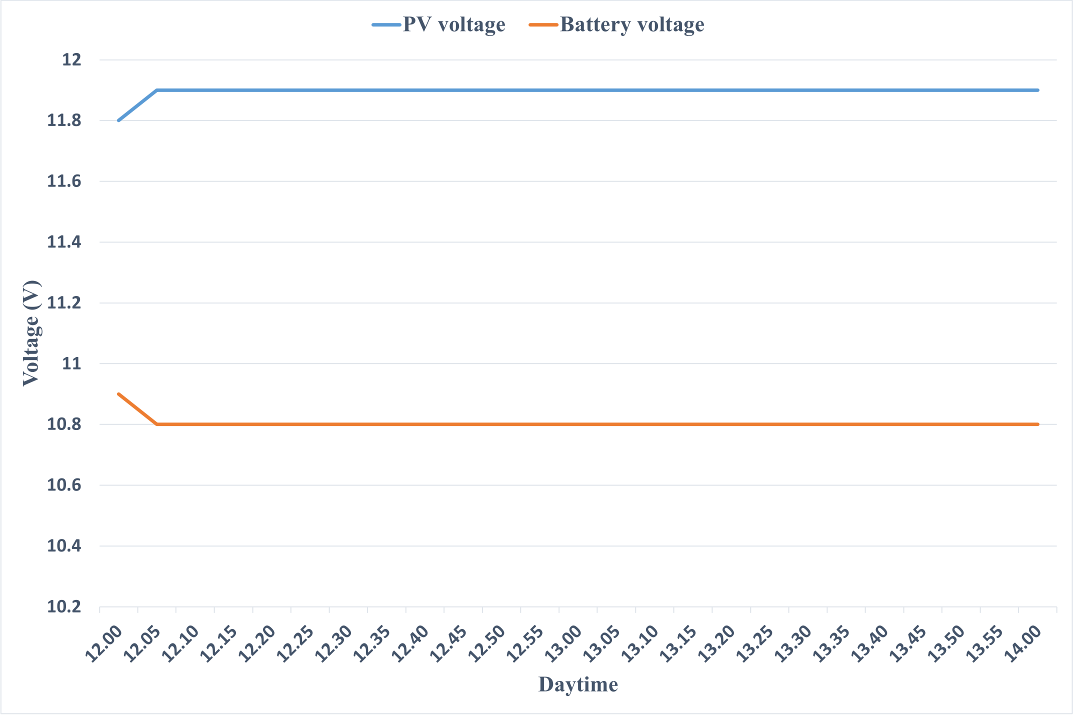

FIGURE 11. PV and battery current against daytime. Both voltages are measured at the output terminal of the MPPT controller.

to the evaporation process. Considering the brine mass (m_{brine}) of 4.5 kg, the temperature was increased (ΔT) from 36 to 79.2 ^{o}C corresponds to a sensible heat gain of approximately 0.81 MJ. In addition, the latent heat

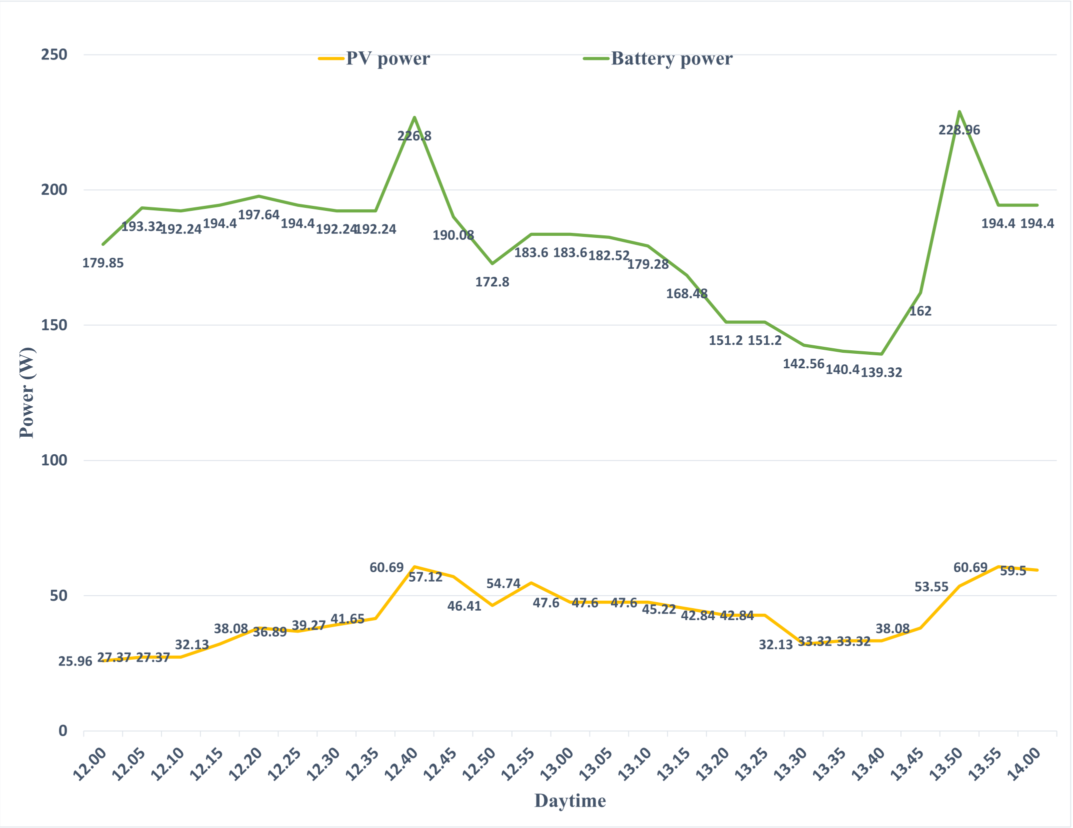

FIGURE 12. Variation of PV power and battery charging power to the glow plug load during daytime operation. The total electrical power and energy supplied to the load was approximately $\sum P_{load} = 4527.93$ W and $\sum P_{load} \times t = 377.3$ Wh, respectively.

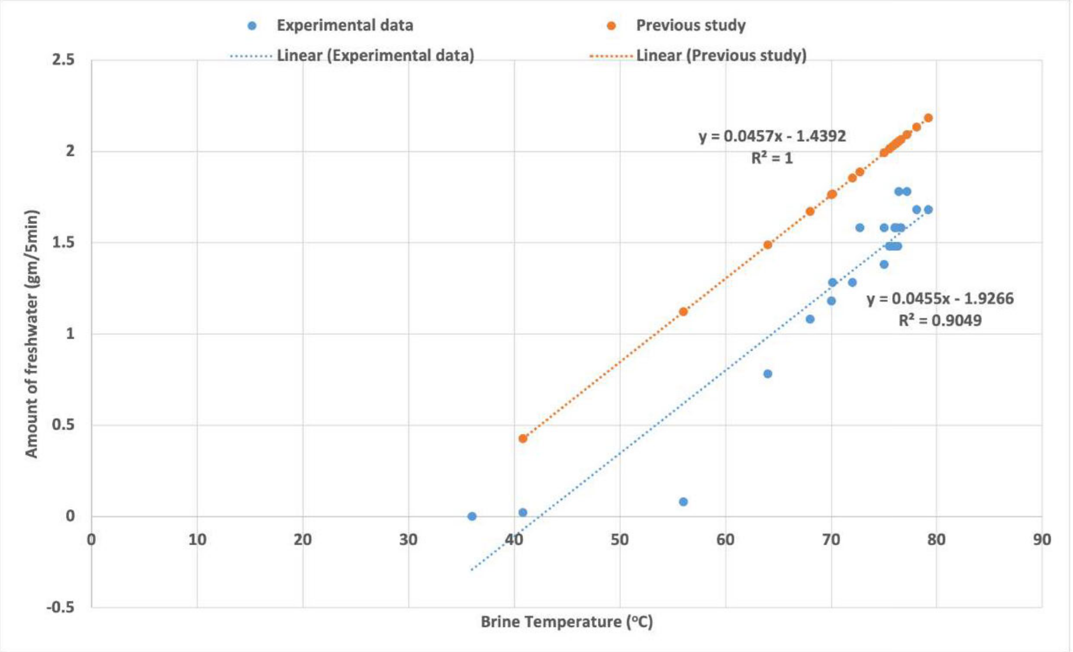

FIGURE 13. Relationship between amount of freshwater production with brine temperature. Experimental data shows linear correlation coefficient with $R^2 = 0.9049$. This trend supports previous study of [47].

associated with the measured freshwater production of 0.032 kg can be calculated approximately 0.075 MJ, based on a latent heat of vaporization (S_l) of 2.35 MJ/kg. The 2.35 MJ/kg is the average of 1st and 2nd hour of latent

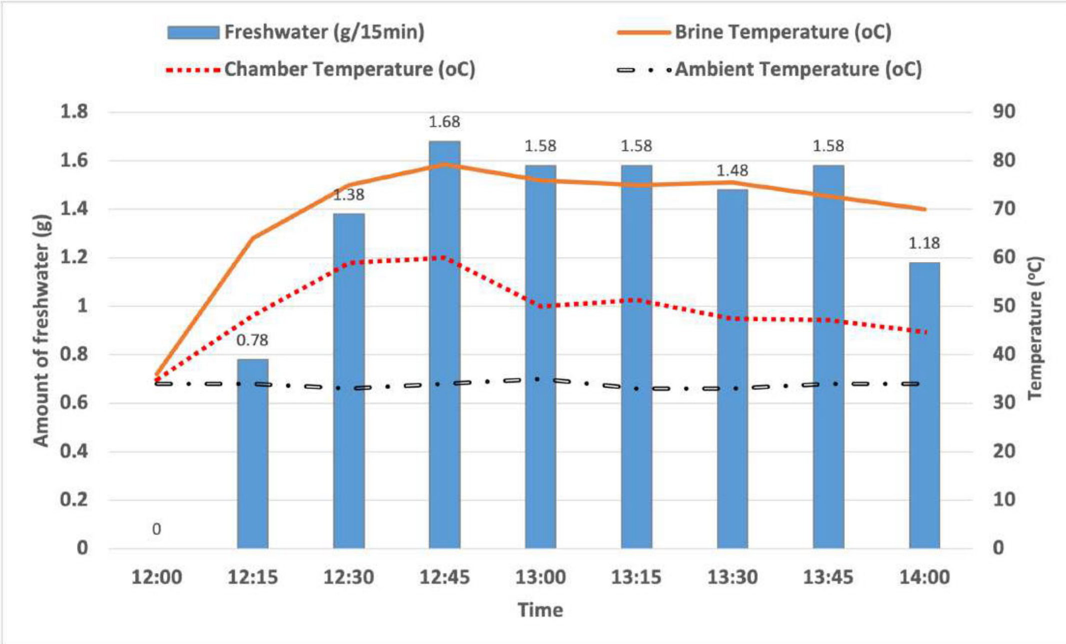

FIGURE 14. Amount of freshwater against ambient, brine, and chamber temperature. Although the ambient temperature was within 33-35 ^{o}C, a maximum of 1.68 g of freshwater production was recorded due to presence of external SPWH system.

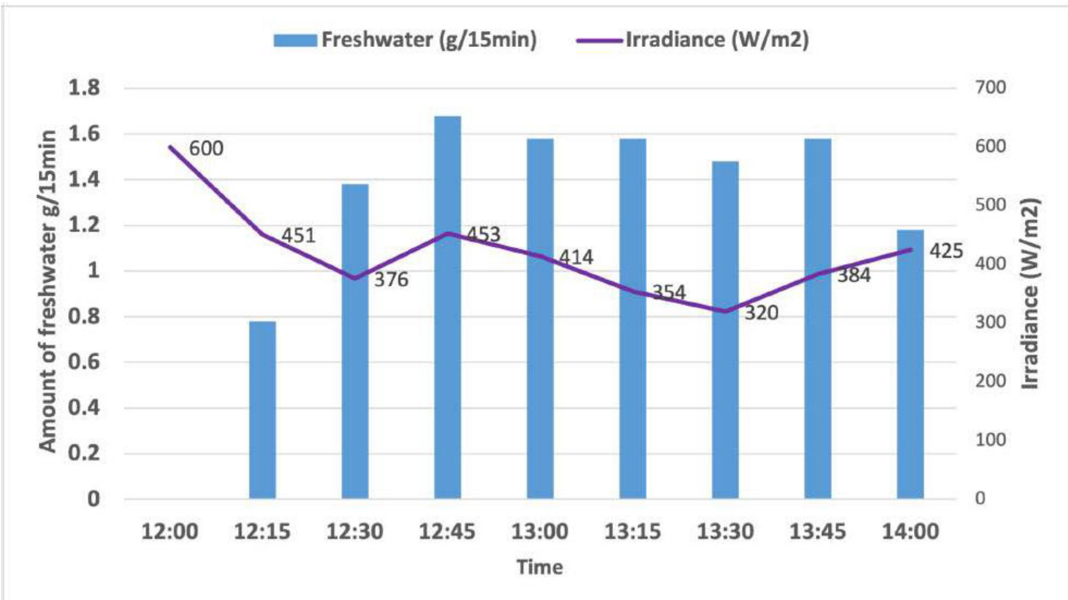

FIGURE 15. Amount of freshwater production against solar irradiance. The SPWH system maintained the steady freshwater production even under cloudy conditions and at irradiance levels below 500 W/m^2.

heat of vaporization, obtained from Eq. 14. Therefore, the combined thermal energy together with water heating and vapor production is found to be 0.882 MJ, representing about 64.71% of the electrical energy supplied to the heater. The remaining portion can be attributed to heat losses through the still structure, convection, and other system inefficiencies. Table 5 shows the calculation for energy balance analysis – electrical energy input into the glow plug vs. thermal gain.

F. WATER QUALITY TEST

During the desalination process, brine water is heated by solar energy together with the glow plug enabled SPWH system. As the water evaporates, salts, heavy metals, and

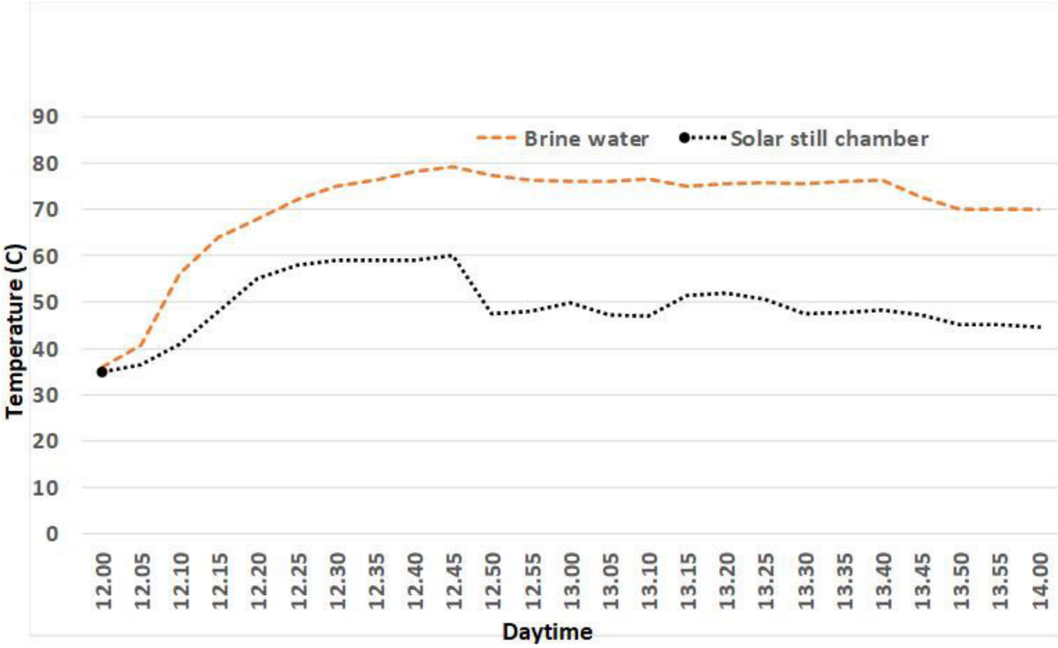

FIGURE 16. Comparison of brine water and solar still chamber temperature. Orange and black dashed lines refer to brine water and solar still chamber temperature, respectively.

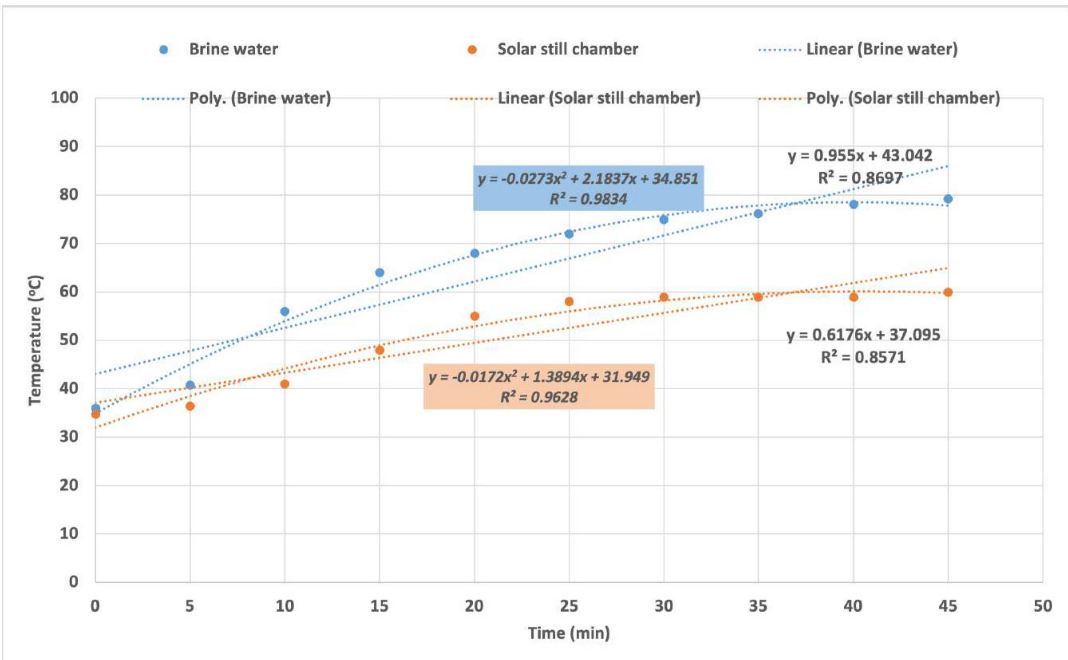

FIGURE 17. Analysis of rate of temperature increase for brine and solar still chamber. It shows strong positive relation and fitted data points with $R^2 = 0.8697$ and $R^2 = 0.8571$, respectively. The polynomial function of order 2 shows more fitted for both temperature profiles with data points of R^2 =0.98.

other contaminants remain in the basin while only water vapor rises and condenses as freshwater. The relatively high operating temperature during the process also helps reduce microbial activity, which contributes to improving the quality of the collected water.

The water quality was tested in explicitly in our previous studies, such as [47] In this study, a self-developed monitoring system containing three sensors—pH, turbidity, and total dissolved solids (TDS)—was employed to evaluate the quality of the collected freshwater. The measured values were

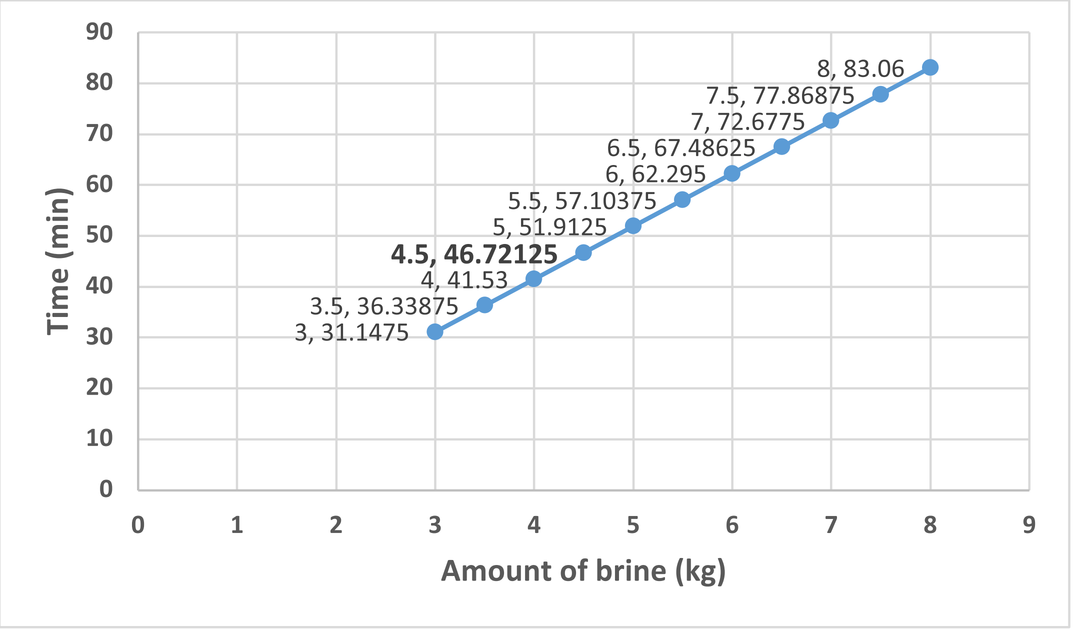

FIGURE 18. Theoretical analysis on required time of brine temperature from 35 to 80 ^{o}C against amount of brine, load power, P_{load} = 300 W, specific heat of the brine, S_b = 4153.0 J/kg.

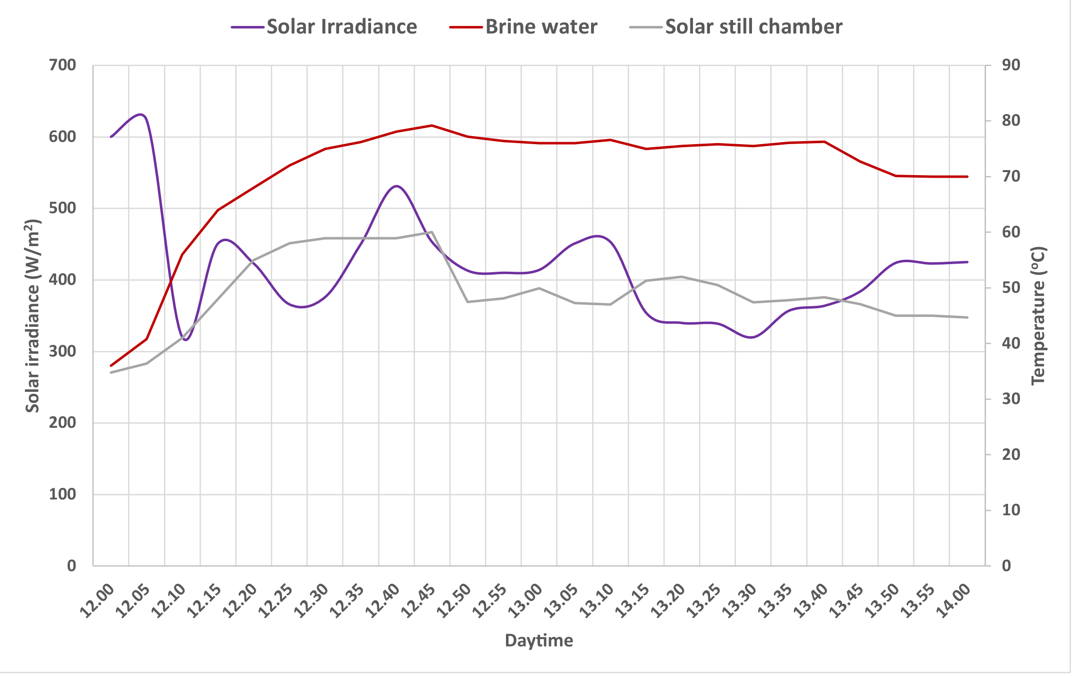

FIGURE 19. Brine water and solar still temperature against solar irradiance throughout daytime.

compared with recommended drinking water limits as well as with results reported in our earlier research. The pH sensor was used to determine the acidity or alkalinity of the product water, and the measured value was 7.3, which falls within the acceptable range for drinking water according to the World Health Organization drinking water guidelines (typically pH 6.5–8.5). Turbidity was measured using a turbidity sensor expressed in Nephelometric Turbidity Units (NTU), which indicates the presence of suspended particles in the water. The recorded turbidity value of the distilled water was 0.7 NTU, which is below the recommended limit of 5 NTU for drinking water. The total dissolved solids (TDS) concentration was measured as 19 ppm, indicating that the concentration of dissolved ions and salts in the product water is very

TABLE 5. Energy balance – electrical energy input into the glow plug vs. thermal gain.

Electrical energy analysis	Thermal energy analysis
$\sum P_{load} = 4527.93$ W Time interval, $t = 5$ min or 0.08 h Total electrical energy, $E_{electrical} = \sum P_{load} \times t = 377.33$ Wh or 1.36 MJ	i. Sensible heat to raise brine temperature Specific heat of the brine at 31 °C, $S_b = 4153.0$ J/kg.K Temperature difference of brine (from 36 to 79.2 °C), ΔT= 43.2 °C Mass of brine, $m_{brine} = 4.5$ kg So, sensible heat $= m_{brine} \times S_b \times \Delta T$ $= 807343.2$ J or 0.81 MJ ii. Latent heat for evaporation Amount of freshwater, $M_{cum} = 0.032$ kg Latent heat of vaporization, $S_l = 2350419.72$ J (from Eq. 14) So, latent heat $= M_{cum} \times S_l = 75213.43$ J Total thermal energy, $E_{thermal}$ =(i) + (ii) = 882556.63 J or 0.88 MJ
Energy utilization percentage	
$\frac{E_{thermal}}{E_{electrical}} = \frac{0.88}{1.36} = 64.71\%$	

TABLE 6. Water quality parameters of the produced freshwater.

Sensors	Recommended range	Description	Tested result
pH	5.5–7.5	Pure water absorbs CO_2 from the air, which slightly reduces its pH.	7.30
Turbidity	< 1 NTU	Turbidity values above 1 NTU may indicate dust, biofilm, or fine droplets splashing from the basin walls.	0.7
TDS	0–50 ppm	Distillation removes more than 99% of salts from seawater; residual TDS mainly comes from dissolved CO_2, trace silicic acid from glass, or minerals leached from tubing.	19

low and well below the commonly recommended limit of 0-50 ppm. Table 6 presents the recommended limits together with the measured values obtained in this study. Based on the comparison with drinking water guidelines and the consistency with results reported in our previous research, the produced water from the solar still can be considered clean and suitable for potable use.

G. COST ESTIMATION

The additional components, namely glow plug, battery, MPPT, and solar PV introduced extra cost to the conventional solar still system. Table 7 presents a breakdown of the cost details for all the components in the developed glow plug with SPWH system.

The solar still, created in the Faculty of Electrical and Electronic Engineering laboratory by our research team, utilizes materials and equipment locally sourced in Malaysia. The financial analysis was conducted using both Malaysian Ringgit (RM) and U.S. dollars (US$), with an exchange rate of RM1.00 equivalent to US$4.68. The comprehensive cost of the SPWH was tallied, encompassing all mechanical and electrical components, amounting to approximately $363.74 (RM1702.30).

Our empirical research posits a 10-year lifespan for the SPWH structure and electrical components, during which maintenance or replacements are anticipated. The transparent plastic cover, for instance, is projected to need replacement every 6 months, amounting to 2 times a year or 18 times over the decade (first year does not require maintenance), at a total cost of $32.69. Other mechanical parts will also require periodic replacement: PVC every 3 years ($10.38 total), the Aluminium composite holder every year ($3.85 total), and Aluminium containers annually ($24.62 total), culminating in a 9-year mechanical maintenance expense of $72.50.

TABLE 7. Cost analysis - initial investment, payback period, CPL, and operating and maintenance.

Category	Item	Cost		Operating and maintenance cost			
		RM (Ringgit Malaysia)	US \$ (\$1= RM4.68)	Replacement frequency Times/year	Cost per year RM	Cost per 9 years RM	Cost per 9 years US\$
Mechanical part	Transparent plastic cover	8.50	1.82	2	17	153	32.69
	PVC for solar still structure	18	3.84	0.30	5.40	48.60	10.38
	Aluminum composite holder	2	0.43	1	2	18.00	3.85
	Hexagon nuts, flange, cramp terminal	1	0.20	0.5	0.5	4.5	0.96
	Aluminum containers	12.80	2.74	1	12.80	115.20	24.62
Subtotal		**42.30**	**9.04**	**-**	**37.7**	**339.30**	**72.5**
Electrical part	12V glow plug	20	4.27	1	20	180.00	38.46
	MPPT	65	13.88	0.50	32.50	292.50	62.50
	Lead acid battery, 100 Ah	700	149.57	0.10	70.00	630.00	134.62
	Solar PV, mono type 425 W	745	159.18	0.00	0.00	0.00	0.00
	Cables	20	4.27	0.50	10.00	90.00	19.23
	Safety switches	10	2.14	0.50	5.00	45.00	9.62
Subtotal		**1560.00**	**333.33**	-	**137.50**	**1237.50**	**264.42**
Others, such as transportation and manufacturing		100	21.37	1	20.00	180.00	38.46
C_t =total cost		1702.3	363.75	-	**195.20**	**1756.80**	**375.38**
CRF=Capital recovery factor i=interest rate n=lifespan	$CRF = \frac{i\times(1+i)^n}{(1+i)^n-1}$ i = 4.5% n = 10 years	0.13	0.03				
C_{FA}= 1st annual cost C_B= Bank charge	$C_{FA} = CRF \times C_t + C_B$ $C_B = 0.005 \times C_t$	223.65	47.79				
$C_{(O\&M)}$=Annual operation and maintenance cost	$C_{(O\&M)} = 0.786 \times C_{FA}$	175.79	37.56				
SFF= Sink fund factor	$SFF = \frac{i}{(1+i)^n-1}$	0.08	0.02				
ASV= Annual salvage value SV =salvage value	$ASV = SFF \times SV$ SV =20%	0.016	0.0035				
C_{TA} = Total annual cost	$C_{TA} = C_{FA} + C_{(O\&M)} - ASV$	399.42	85.35				
Daily yield (kg/day)		3.35					
Annual yield (kg/year)	*Daily yield* × 0.8 × 365	978.20					
Inflow amount	*Annual yield* × 0.20 \$/kg	915.60	195.64				
Payback period (year)	$\frac{C_t}{Inflow\ amount}$		1.9				
CPL= Cost per liter	$CPL = \frac{C_{TA}}{Annual\ yield}$	0.41	0.09				

Electrical components, including the glow plug, MPPT, safety switch, and others, are estimated to need annual replacement, summing up to \$264.42 over 9 years. The battery, guaranteed by the manufacturer for 5 years, is expected to be replaced once within the decade. Maintenance for the solar PV is not accounted for, as its warranty exceeds 10 years. Others, such as transportation and manufacturing cost is estimated \$4.27 per year from the second year. Consequently, the total maintenance cost for a decade of operation is calculated to be \$375.38.

The total capital cost (C_t) is the summation of all initial costs including electrical, mechanical, and manufacturing and transportation costs. Capital recovery factor (CRF) is obtained from Eq. 20, where interest rate (i) in Malaysia is 4.5% for period of 10 years ($n = 10$). We also consider one off bank loan processing charge (C_B) as 0.5% of capital cost, C_t. Then we obtain First annual cost (C_{FA}) from Eq. 21 and Eq. 22. This shows capital cost (C_t) and first annual cost (C_{FA}) of \$363.75 and \$47.79 respectively.

$$CRF = \frac{i \times (1+i)^n}{(1+i)^n - 1} \tag{20}$$

$$C_{FA} = CRF \times C_t + C_B \tag{21}$$

$$C_B = 0.005 \times C_t \tag{22}$$

The annual operating and maintenance cost ($C_{(O\&M)}$) is determined by averaging the 10-year cost, representing approximately 0.785% of the first annual cost (C_{FA}). As maintenance is not required in the first year, the total

TABLE 8. Comparison among the previous researchers' outcomes and proposed glow plug in terms of daily yield, max brine temperature, and ambient temperature.

Method & Ref	Country, Year	Yield/day (L/m^2)	Ambient Avg. [W/m^2, ^oC]	Max Brine Temp (^oC)	Rate of Temp Increase (Brine) (^oC/min)	Rate of Temp Increase (Chamber) (^oC/min)	Efficiency (%)	Cost
Solar air heater [21]	Saudi Arabia, 2016	1.3–22	NA, 14–26	42.2	–	0.046	–	0.012 $\$/L/m^2$
Double-gazed [53]	Iran, 2022	1.1	1000, 35	70	0.12	0.12	-	0.10 $\$/L/m^2$
Stepped solar [10]	India, 2022	2.7	800, 30	65	0.06	-	-	-
Inclined tabular [49]	Ha'il, KSA, 2022	4.42	600, 37	89.3	0.14	0.15	35.62	0.01 $\$/L/m^2$
Typical method [23]	Perak, Malaysia, 2014	2.0	NA, 33	53	0.15	0.067	-	-
Twin wedge [11]	Tamil Nadu, India, 2022	3.61	754, 29–31	54	0.152	0.152	-	0.53 $/day
PCM [54]	KSA, 2024	2.88	-	68	0.125	0.125	-	-
PCM heat storage [52]	6 cities, Morocco, 2023	6.27–11.5	998.19–1023.03, 25.63–41.13	66.03–75.67	0.127–0.154	-	49.04–84.62	-
SS TEG [57]	Iran, 2023	0.63–0.796	500	55	0.10	-	41.8	0.20 $/L
Typical [20]	Egypt 2020	0.03–3.0	966.42–1420, 39.5	63	0.056	-	-	-
Carbon black thin film [46]	Egypt 2022	6.1	552.2, 33	68.3	-	0.11	23.18–82.16	0.02 $/L
Typical [55]	California 2022	5	-	80	0.15	-	-	6.89 $\$/m^3$
Composite [51]	KSA 2021	4.9	600.14, 28–42.5	97	0.37	0.41	20.1	0.02 $/L
Hybrid [56]	India 2011	<2.0	992.3, 984.3, 35.6	60.1	0.204	-	29.96	-
Proposed glow plug with SPWH	**Johor, Malaysia**	**3.35**	**418.6, 33.96**	**79.2**	**0.96**	**0.62**	**49.83-68.18**	**0.09 $\$/kg/m^2$**

$C_{(O\&M)}$ is estimated for the subsequent 9 years, totaling \$375.38. Therefore, the annual $C_{(O\&M)}$ is calculated as the 10-year average of \$375.38, resulting in an annual $C_{(O\&M)}$ of \$37.54.

Total number of low, medium, and high luminance days in Malaysia are 20%, 60%, and 20% of the year respectively, obtained from our previous research [39]. This estimates 80% or 292 days of medium and high luminance days yielding 978.2 kg of freshwater as a annual yield and 9782 kg during the 10-year lifetime.

The production cost per liter (CPL) is determined through Eq. 23. Assuming a freshwater price of \$0.20 per kg, the annual cash inflow is computed at \$195.64 based on the total annual yield. The payback period is then calculated using the averaging method, obtained by dividing the annual cash inflow (\$195.64) by the capital cost (C_t) of \$363.75. Consequently, the payback period is found to be 1.9 years. The cost analysis follows the methodology outlined by Ref. [49], [50] shown in Table 7.

$$CPL = \frac{C_{TA}}{Annual\ yield} \tag{23}$$

H. DISCUSSION AND COMPARISON

To assess the findings of this study, an analysis is performed comparing them with the latest relevant research. Table 8 outlines the key results of this study and other related works. Since the integration of glow plug with SPWH is novel, no similar publications have been found in the literature. As a result, the comparative approach involves evaluating the outcomes of this study against the most relevant publications in the areas of solar air heaters, double-glazed systems, stepped solar designs, inclined tabular configurations, twin-wedge setups, phase change material, and hybrid systems.

Comparison analysis indicates that daily freshwater yield varies by location and solar irradiance, structure of the solar still, and volume of brine in the container. However, the most dominant factor contributing to higher yield is high solar irradiance, which in turn stimulates the evaporation rate by increasing the temperature of the brine water. Referring to Table 8, the overall yield per day of this study is comparatively lower than a few researchers by 31.9 [49], 46.26 [51], and 87% [52]. The lower yield achieved by this current study is attributed to both the typical structure of the solar still chamber, moderate level of solar irradiance, and 0 m/s of wind speed. In [52], the results from theoretical approach showed that higher wind speeds could lead to increased production, with a range of 6.27-11.5 L/m^2 of freshwater per day. In [51], a heat storage composite system is used to enhance the brine and chamber temperature that increased freshwater yield to 4.9 L/m^2.

All the previous studies conducted experiments during the Summer at 8.00 AM, and we observed that no vaporization occurred until the chamber temperature reached 40 ^oC. This implies that it took nearly 2 hours to raise the brine temperature from the initial level to 40 ^oC. In this study, by employing a glow plug, the chamber temperature reached 40 ^oC within 5 minutes and 80 ^oC within 45 minutes. Therefore, the rate of temperature increase (^oC/min) of brine in this study is found to be 6-8 times higher than that in previous studies, referred in [10], [23], [49], [52], [53], [54], [55], [56] and more than 10 times higher than [9], [19], [57]. When comparing with the chamber temperature, the current study outperforms, Refs. [10], [20], [23], [49], [53], [54], by 5 to 13 times. This has resulted in an average system efficiency improvement of 57.94%, surpassing all previous studies except for theoretically analyzed Ref. [52] and nano-enhanced energy storage material (23.18-82.16%) Ref. [46], to the best of our knowledge. The key benefit of the proposed system lies in its ability to substantially elevate both the brine and chamber temperatures from the beginning of the day, which is one of the crucial factors influencing the system efficiency. We also observe a significant improvement in efficiency in previous studies using extra materials and techniques in methods, such as inclined and tubular solar still with parabolic concentrator (35.62% improvement) [51], solar still thermoelectric generator or SS TEG (41.8% improvement) [57], and hybrid solar still as a co-generative system (29.96% improvement) [56]. Sai Kiran Hota et al. found carbon black particles as inexpensive for a small community water solution [55]. When comparing the cost per liter (*CPL*), we observed variations in the consideration of different interest rates by various researchers, such as 15% in some locations and 6% in KSA. Consequently, the *CPL* calculation lacks uniformity. In our research, we determined the *CPL* to be \$0.09/kg, based on a 4.5% interest rate in Malaysia.

Although humidity and other environmental conditions vary between locations, the evaporation rate highly depends on the solar still chamber and brine temperature. This temperature is found to be influenced by solar irradiance and the structure of the solar still chamber. Therefore, in this research, we utilized solar irradiance to increase the chamber temperature and power the glow plug for heating the brine. The solar-powered glow plug serves as an additional heating element to enhance the efficiency of the desalination system. This element can rapidly increase the brine temperature, leading to a shorter desalination period. Referring to Table 8, the proposed system has achieved a brine temperature as high as 79.2 ^{o}C - the highest among previous researchers, despite having a lower average day irradiance compared to the location of previous research.

IV. CONCLUSION

This study focuses on the design and model of a new glow plug-integrated solar still desalination technique to improve the evaporation rate. We investigated the electrical and economic impact of the glow plug in an inclined solar still desalination system powered by a solar PV. The objective of this study is to raise the brine temperature inside the solar still chamber by converting electrical energy into heat. The inclusion of the glow plug has significantly improved the overall performance of the system. To accommodate the 300 W load of the glow plug, the power requirements were calculated to optimize the size of the PV system and battery. Considering load current of 25 A, appropriate cables, MPPT charge controller, and switches were selected using mathematical models. The finalized system specifications consist of a 425 W PV array, a 12 V 100 Ah lead acid deep cycle battery, a 30 A DC switch, and a 75 V 50 A MPPT charge controller. These selections guarantee a stable voltage supply to the battery, with a fluctuation rate of less than 0.9%. The system size is designed to effectively mitigate potential issues caused by extensive cloud coverage and days with moderate luminance. This ensures uninterrupted power supply to the glow plug, sustaining the rise in brine temperature even under fluctuating irradiance conditions commonly found in climates like Malaysia. From battery sizing analysis, we observed that maximizing the load hours per day can be more economically viable compared to increasing the number of autonomous days.

The major findings of this research can be summarized based on the investigation results:

- Almost no vapor was observed in the still initially at 500 W/m^2 irradiance and 25 ^{o}C ambient temperature. Because time is required for the chamber to reach a certain temperature to initiate evaporation.
- Based on the system modeling and *autonomous day* = 1, we obtained optimal sizing of electrical components-cables: 12 AWG, solar PV: 166 W, battery: 84 Ah, and MPPT: 29 A. The system efficiency is determined above and below 70 ^{o}C based on the ratio of output energy (freshwater production) and input solar radiation energy.
- The average solar irradiance and ambient temperature were measured at 418.56 W/m^2 and 33.96 ^{o}C, respectively. The standard deviation for temperature and irradiance are 0.53 (less disperse) and 76.84 (high disperse from mean), respectively. The fluctuated 6-8 oktas cloud cover causes switch variations in solar irradiance, which are mitigated by appropriate battery sizing.
- The glow plug enabled SPWH can raise the brine and still chamber temperature to 79.2 ^{o}C and 60 ^{o}C within 45 minutes. It requires 840.98 kJ of energy conversion for a 4.5 kg brine. For this conversion, SPWH consumes up to 21.2 A current. By supplying this high amount of current from the battery can cause it to be fully drained out of it, it is suggested to use a controller for using SPWH. Both battery and load voltage shifts were found to be 0.9%, which complies with the voltage regulation limit of ± 5% as specified in IEC 60038.
- The temperature profile indicates that brine water heats up more rapidly than the solar still chamber, reaching a peak of about 79.2 ^{o}C, while the chamber peaks near 56 ^{o}C. Brine temperature remains relatively stable with minimal fluctuations (±2 ^{o}C), ideal for sustained evaporation. In contrast, the chamber temperature shows greater variability. The increasing temperature difference between brine and chamber— from 22 ^{o}C to 28 ^{o}C —suggests better heat retention in the brine, attributed to its higher specific heat capacity and possible convective or radiative losses from the chamber.
- The rate of temperature increase for the brine was determined to be 0.96 ^{o}C/min, while for the solar still chamber, it was found to be 0.62 ^{o}C/min. These values were derived through rigorous regression analysis using

the best-fitted models, resulting in an R^2 value of 0.87, surpassing previous research.

- The average brine temperature recorded was 70.58 °C, yielding freshwater production of 0.032 kg / 0.043 m^2 in 2 hours under the climate conditions of Malaysia.
- The achieved productivity and the highest thermal efficiency of the SPWH system are 3.35 L/day/m^2 and 68.18%, respectively. The efficiency is improved by reducing the waiting time for initiating vaporization.
- The cost per liter (*CPL*) for this system is reduced to a competitive level of $0.09/kg per m^2, accounting for a 4.5% interest rate.
- The inclusion of glow plug in the desalination system demonstrated higher performance compared to other solar desalination systems under tropical climates.

The limitation of this study is that the experiments were conducted over a short operating period and therefore long-term durability aspects such as corrosion rate, sheath leakage, and scale formation were not quantitatively evaluated. It is acknowledged that saline environments may promote corrosion and scaling depending on brine composition and operating duration. In the current prototype, periodic visual inspection and manual cleaning of the heater surface were carried out to remove salt deposits.

Although daily water production was moderate due to ambient conditions, reaching nearly 80 °C brine temperature marks a significant improvement over previous studies. In future work, the authors intend to study the performance of the proposed glow plug enabled SPWH in a large commercial scale using an improved design for the solar still chamber.

ACKNOWLEDGMENT
The authors would like to thank Keshika A/P Manimaran for conducting the freshwater quality test.

ACRONYMS

T	Temperature (°C).
R	Resistance (Ω).
t	time (s).
m	Mass (kg).
S	Specific heat (J/kg.K).
P	Power (W).
I	Current (A).
L	Cable distance (feet).
V	Voltage (V).
E	Energy (Wh).
h	Hour (h).
S_h	Sun hour (h).
N	Number.
CB	Battery capacity (Ah).
B	Battery loss (%).
M_{cum}	Amount of total freshwater productivity (kg).
A	Area of solar still (m^2).
Z	Average solar irradiance (W/m^2).
CRF	Capital recovery factor.
i	Interest rate (%).
n	Lifespan (years).
C	Cost.
SFF	Sink fund factor.
ASV	Annual salvage value.
SV	Salvage value.
CPL	Cost per liter.

A. GREEK SYMBOLS

k	Constant.
η	System efficiency (%).

B. SUBSCRIPTS

i	Initial.
f	Final.
b	Brine.
pv	Photovoltaic or PV.
max	Maximum.
oc	Open circuit.
mpp	Maximum power point.
sc	Short circuit.
bat	Battery.
nom	Nominal.
DoD	Depth of discharge.
oc, r	Rated open circuit voltage.
mc	Maximum charge.
bc	Battery charge.
l	Latent heat.
amb	Ambient.
t	Total.
FA	First annual.
B	Bank.
$O\&M$	Operation and maintenance.
TA	Total annual.
sys	System.
$load$	System load.

REFERENCES

[1] A. Ahsan, T. Ahmed, M. A. Uddin, A. O. Al-Sulttani, M. Shafiquzzaman, M. R. Islam, M. S. Ahmed, Alamin, M. Mohadesh, M. N. Haque, M. Al-Mutiry, and A. Masria, "Evaluation of water quality index (WQI) in and around Dhaka city using groundwater quality parameters," *Water*, vol. 15, no. 14, p. 2666, Jul. 2023.

[2] Z. Hu, J. Wang, E. Huo, and C. Zhang, "Investigation of a distillation desalination system driven by solar and ocean thermal energy," *Desalination*, vol. 559, Aug. 2023, Art. no. 116649.

[3] A. Bamasag, E. Almatrafi, T. Alqahtani, P. E. Phelan, M. Ullah, M. Mustakeem, M. Obaid, and N. Ghaffour, "Recent advances and future prospects in direct solar desalination systems using membrane distillation technology," *J. Cleaner Prod.*, vol. 385, Dec. 2022, Art. no. 135737.

[4] T. Arunkumar, R. Jayaprakash, D. Denkenberger, A. Ahsan, M. S. Okundamiya, S. Kumar, H. Tanaka, and H. Aybar, "An experimental study on a hemispherical solar still," *Desalination*, vol. 286, pp. 342–348, Feb. 2012.

[5] C. Payus, L. A. Huey, F. Adnan, A. B. Rimba, G. Mohan, S. K. Chapagain, G. Roder, A. Gasparatos, and K. Fukushi, "Impact of extreme drought climate on water security in north borneo: Case study of sabah," *Water*, vol. 12, no. 4, p. 1135, Apr. 2020.

[6] P. Pal, R. Dev, D. Singh, and A. Ahsan, "Energy matrices, exergoeconomic and enviroeconomic analysis of modified multi–wick basin type double slope solar still," *Desalination*, vol. 447, pp. 55–73, Dec. 2018.

[7] J. N. Easley, S. Talozi, and A. G. Winter V., "Feasibility and design of solar-powered electrodialysis reversal desalination systems for agricultural applications in the Middle East and North Africa," *Desalination*, vol. 561, Sep. 2023, Art. no. 116628.

[8] G. Gopi, G. Arthanareeswaran, and A. Ismail, "Perspective of renewable desalination by using membrane distillation," *Chem. Eng. Res. Design*, vol. 144, pp. 520–537, Apr. 2019.

[9] M. R. Qtaishat and F. Banat, "Desalination by solar powered membrane distillation systems," *Desalination*, vol. 308, pp. 186–197, Jan. 2013.

[10] S. Pal, A. Dixit, B. Raj, K. Pal, G. Saiprakash, S. C. Ram, and A. Gautam, "Comparative study of performance measure of modified stepped solar still with conventional solar still for water desalination processes," in *Proc. 2nd Int. Conf. Innov. Sustain. Comput. Technol. (CISCT)*, Dec. 2022, pp. 1–6.

[11] A. W. Jeevadason, S. Padmini, and C. Bharatiraja, "Enhancing freshwater productivity of twin wedge solar still by temperature control through thermoelectric sensors and modules," *IEEE Sensors J.*, vol. 22, no. 9, pp. 9095–9103, May 2022.

[12] A. A. A. Abuelnuor, A. A. M. Omara, H. M. H. Musa, S. M. Abaza, M. A. E. Adam, and M. O. O. Abdalraheem, "Experimental study on solar still desalination system integrated with solar collector and phase change material," in *Proc. Int. Conf. Comput., Control, Electr., Electron. Eng. (ICCCEEE)*, Feb. 2021, pp. 1–5.

[13] T. Arunkumar, D. Denkenberger, A. Ahsan, and R. Jayaprakash, "The augmentation of distillate yield by using concentrator coupled solar still with phase change material," *Desalination*, vol. 314, pp. 189–192, Apr. 2013.

[14] M. Bouzaid, O. Ansari, M. Oubrek, and M. Taha-Janan, "Experimental analysis of an inclined cascade solar still with slope surfaces and baffles," in *Proc. Int. Renew. Sustain. Energy Conf. (IRSEC)*, Dec. 2017, pp. 1–5.

[15] S. Kumaravel., M. Nagaraj, and G. Bharathiraja., "Study on the performance of single slope solar still using marble stone as energy storage material," in *Proc. 5th Int. Conf. Smart Syst. Inventive Technol. (ICSSIT)*, Jan. 2023, pp. 278–283.

[16] M. M. Gamaleldin, S. M. Elsherbiny, S. Zenhom Ibrahim, and O. A. El Samni, "Performance analysis of successive evaporation condensation solar still (SECSS) desalination unit with heat recovery," in *Proc. 12th Int. Renew. Eng. Conf. (IREC)*, Apr. 2021, pp. 1–6.

[17] E. Rubio, "Monolithic solar stills: A new approach for manufacturing of water desalination products," *IEEE Latin Amer. Trans.*, vol. 13, no. 10, pp. 3338–3342, Oct. 2015.

[18] T. Arunkumar, R. Velraj, D. C. Denkenberger, R. Sathyamurthy, K. V. Kumar, and A. Ahsan, "Productivity enhancements of compound parabolic concentrator tubular solar stills," *Renew. Energy*, vol. 88, pp. 391–400, Apr. 2016.

[19] H. A. Maddah, "Predictive regression models for solar energy harvesting and sustainable, low energy, highly efficient solar-desalination systems," in *Proc. 5th Int. Conf. Power Energy Eng. (ICPEE)*, Dec. 2021, pp. 111–115.

[20] M. Mostafa, H. M. Abdullah, and M. A. Mohamed, "Modeling and experimental investigation of solar stills for enhancing water desalination process," *IEEE Access*, vol. 8, pp. 219457–219472, 2020.

[21] F. R. Siddiqui, N. A. S. Elminshawy, and M. F. Addas, "Design and performance improvement of a solar desalination system by using solar air heater: Experimental and theoretical approach," *Desalination*, vol. 399, pp. 78–87, Dec. 2016.

[22] A. Ahsan, N. S. Ahmad, A. Riahi, M. Alhaz Uddin, D. N. Hridoy, M. Shafiquzzaman, M. Imteaz, S. Idrus, N. Al-Ansari, M. A. U. R. Atiq, and A. Ng, "Modeling of a new triangular shape solar distillation system integrated with solar PV panel and DC water heater," *Case Stud. Thermal Eng.*, vol. 44, Apr. 2023, Art. no. 102843.

[23] M. Khir and A. Raziqin. (2014). *Optimization of Solar Still for Potable Water Production Using Double Slope*. [Online]. Available: http://utpedia.utp.edu.my/id/eprint/14072/1/AHMAD%20RAZIQIN15200%20Dissertation.pdf

[24] Y. Alfaifi, H. Qudrah, N. Alnuaim, M. Aldeghreer, and M. Alshammari, "Solar water heater geyser," Dept. of Mechanical Engineering, Prince Mohammad Bin Fahd Univ., Saudi Arabia, Tech. Rep. 21, 2021. [Online]. Available: https://www.pmu.edu.sa/attachments/academics/pdf/udp/coe/dept/me/12-solar-water-heater-geyser.pdf

[25] A. Elsheikh, M. Zayed, A. Aboghazala, F. A. Essa, S. Rehman, O. L. Muskens, A. Kamal, and M. A. Elaziz, "Innovative solar distillation system with prismatic absorber basin: Experimental analysis and LSTM machine learning modeling coupled with great wall construction algorithm," *Process Saf. Environ. Protection*, vol. 186, pp. 1120–1133, Jun. 2024.

[26] M. E. H. Attia, A. E. Kabeel, M. E. Zayed, M. Arıcı, and M. Abdelgaied, "Optimal size of spherical rock salt balls as low-cost thermal storage materials for performance augmentation of hemispherical solar distillers: Experimental investigation and thermo-economic analysis," *J. Cleaner Prod.*, vol. 374, Nov. 2022, Art. no. 134006.

[27] M. El Hadi Attia, M. E. Zayed, A. E. Kabeel, M. Abdelgaied, M. Arıcı, and M. M. Abdel-Aziz, "A comparative experimental study on hemispheric distillation system integrated with metamorphic fabric materials for efficient and low-cost solar desalination," *Thermal Sci. Eng. Prog.*, vol. 47, Jan. 2024, Art. no. 102277.

[28] M. Abdelgaied, M. E. H. Attia, A. E. Kabeel, and M. E. Zayed, "Improving the thermo-economic performance of hemispherical solar distiller using copper oxide nanofluids and phase change materials: Experimental and theoretical investigation," *Sol. Energy Mater. Sol. Cells*, vol. 238, May 2022, Art. no. 111596.

[29] F. A. Hammad, M. E. Zayed, E. El-Bialy, K. Irshad, Z. Lu, and S. M. Shalaby, "Performance assessment of a novel solar distiller with a fountain-shaped basin design embedded with phase change materials enriched with copper oxide nano-additives: A detailed experimental investigation," *J. Energy Storage*, vol. 82, Mar. 2024, Art. no. 110555.

[30] F. A. Hammad, S. M. Shalaby, and M. E. Zayed, "Innovative design of a dome-shaped solar distiller enhanced with a multi-tray conical absorber basin and fountain feeding supply: Experimental study with energy, exergy, and enviro-economic analyses," *Sol. Energy*, vol. 266, Dec. 2023, Art. no. 112183.

[31] M.-W. Wang, R.-Y. Hsu, C.-F. Hung, and T.-C. Cheng, "Performance enhancement of a small solar desalination still with active solar tracking, spray evaporation, and auxiliary electrical heating," *Case Stud. Thermal Eng.*, vol. 79, Mar. 2026, Art. no. 107792.

[32] D. P. Pandara, A. Ardiansyah, G. Pasau, V. A. Suoth, G. H. Tamuntuan, M. A. Laoh, R. A. Abudu, H. F. Sangian, and D. Tahir, "Enhanced solar desalination performance via integrated interfacial heating and PV-assisted water circulation in a modified single-slope solar still," *Results Eng.*, vol. 27, Sep. 2025, Art. no. 105700.

[33] A. Pacheco, C. Sequeira, M. Moreira da Silva, and V. S. Sousa, "Enhancing efficiency in solar non-intrusive desalination: Solar still prototype optimization in Southwest Europe," *Desalination*, vol. 598, Apr. 2025, Art. no. 118421.

[34] N. A. S. Elminshawy, F. R. Siddiqui, and M. F. Addas, "Experimental and analytical study on productivity augmentation of a novel solar humidification–dehumidification (HDH) system," *Desalination*, vol. 365, pp. 36–45, Jun. 2015.

[35] A. Abdulsalam, A. Idris, T. A. Mohamed, and A. Ahsan, "An integrated technique using solar and evaporation ponds for effective brine disposal management," *Int. J. Sustain. Energy*, vol. 36, no. 9, pp. 914–925, Oct. 2017.

[36] U. Sorfina, S. Z. Islam, K. B. Ching, D. M. Soomro, and J. A.-F. Yahaya, "Adaptive position control of DC motor for brush-based photovoltaic cleaning system automation," *Bull. Electr. Eng. Informat.*, vol. 12, no. 3, pp. 1293–1301, 2023.

[37] U. Shahira, S. Z. Islam, R. Omar, M. L. Othman, S. Z. Said, and J. Uddin, "Electrical design of solar-powered recreational boat in Malaysia," in *Proc. IEEE Int. Conf. Power Energy (PECon)*, Dec. 2022, pp. 138–143.

[38] S. Z. Islam, N. S. Izzati, M. N. Abdullah, M. S. Kamarudin, R. Omar, and J. Uddin, "Automated water recycle (AWR) method for dust removal from rooftop photovoltaic (PV) at Johor, Malaysia," *Social Netw. Appl. Sci.*, vol. 4, no. 11, p. 321, Nov. 2022.

[39] S. Z. Islam, M. L. Othman, M. Saufi, R. Omar, A. Toudeshki, and S. Z. Islam, "Photovoltaic modules evaluation and dry-season energy yield prediction model for NEM in malaysia," *PLoS ONE*, vol. 15, no. 11, Nov. 2020, Art. no. e0241927.

[40] T. Zhou, C. Yao, Y. Hu, F. Yang, J. Wang, and M. Ouyang, "Research on performance and temperature control of glow plugs for PPCI low load assist," *IFAC-PapersOnLine*, vol. 49, no. 11, pp. 223–230, 2016.

[41] M. Özcan, M. F. Ünlerşen, and M. Şen, "Determination of optimum design parameters of glow plug and experimental verification," *Turkish J. Eng.*, vol. 7, no. 2, pp. 125–133, Apr. 2023.
[42] L. Zhao, J. Lei, Y. Liu, W. Deng, and L. Yang, "Energy-based cold-start strategies for diesel engines at extreme low temperature," *Thermal Sci. Eng. Prog.*, vol. 47, Jan. 2024, Art. no. 102274.
[43] A. Ramalingam and S. Arumugam, "Experimental study on specific heat of hot brine for salt gradient solar pond application," *Int. J. ChemTech Res*, vol. 4, no. 3, pp. 956–961, 2012.
[44] S. Z. Islam, M. S. B. Kamarudin, M. N. B. Abdullah, M. Mohaffyza, L. C. Sern, M. L. Othman, and J. Uddin, "Sustainable smart irrigation system (SIS) using solar PV with rainwater harvesting technique for indoor plants," *PLoS ONE*, vol. 20, no. 3, Mar. 2025, Art. no. e0316911.
[45] M. S. Yousef, H. Hassan, and H. Sekiguchi, "Energy, exergy, economic and enviroeconomic (4E) analyses of solar distillation system using different absorbing materials," *Appl. Thermal Eng.*, vol. 150, pp. 30–41, Mar. 2019.
[46] S. W. Sharshir, A. W. Kandeal, Y. M. Ellakany, I. Maher, A. Khalil, A. Swidan, G. B. Abdelaziz, H. Koheil, and M. Rashad, "Improving the performance of tubular solar still integrated with drilled carbonized wood and carbon black thin film evaporation," *Sol. Energy*, vol. 233, pp. 504–514, Feb. 2022.
[47] N. Y. Y. Emran, A. Ahsan, E. H. H. Al-Qadami, M. M. El-Sergany, M. Shafiquzzaman, M. Imteaz, A. W. M. Ng, M. A. U. R. Tariq, S. Idrus, Z. Mustaffa, and F. Y. Teo, "Efficiency of a triangular solar still integrated with external PVC pipe solar heater and internal separated condenser," *Sustain. Energy Technol. Assessments*, vol. 52, Aug. 2022, Art. no. 102258.
[48] A. Ahsan, M. Imteaz, U. A. Thomas, M. Azmi, A. Rahman, and N. N. N. Daud, "Parameters affecting the performance of a low cost solar still," *Appl. Energy*, vol. 114, pp. 924–930, Feb. 2014.
[49] M. M. Z. Ahmed, F. Alshammari, I. Alatawi, M. Alhadri, and M. Elashmawy, "A novel solar desalination system integrating inclined and tubular solar still with parabolic concentrator," *Appl. Thermal Eng.*, vol. 213, Aug. 2022, Art. no. 118665.
[50] P. Pal, P. Yadav, R. Dev, and D. Singh, "Performance analysis of modified basin type double slope multi–wick solar still," *Desalination*, vol. 422, pp. 68–82, Nov. 2017.
[51] M. Elashmawy and M. M. Z. Ahmed, "Enhancing tubular solar still productivity using composite aluminum/copper/sand sensible energy storage tubes," *Sol. Energy Mater. Sol. Cells*, vol. 221, Mar. 2021, Art. no. 110882.
[52] H. Hafs, O. Ansari, and A. Bah, "Impact of wind-driven mixed convection on the performance of passive solar desalination with PCM heat storage in varied Moroccan climates," *Ecological Frontiers*, vol. 44, no. 1, pp. 73–83, Feb. 2024.
[53] S. Khanmohammadi, S. Khanjani, and F. Musharavati, "Experimental study and economic examination of double-glazed solar still desalination with a thermoelectric cooling system," *Sustain. Energy Technol. Assessments*, vol. 54, Dec. 2022, Art. no. 102854.
[54] J. Seifi, H. Samimi-Akhijahani, and P. Salami, "Investigating the thermo-economic performance and modeling of a parabolic solar collector with phase change material in the receiver tube in a solar desalination," *Desalination*, vol. 572, Mar. 2024, Art. no. 116980.
[55] S. K. Hota, S. S. Hada, C. Keske, and G. Diaz, "Feasibility of desalination by solar stills for small community scale freshwater demand," *J. Cleaner Prod.*, vol. 379, Dec. 2022, Art. no. 134595.
[56] D. Shukla and K. Modi, "Hybrid solar still as a co-generative system and desalination system–an experimental performance evaluation," *Cleaner Eng. Technol.*, vol. 2, Jun. 2021, Art. no. 100063.
[57] S. Shoeibi, M. Saemian, S. M. Parsa, M. Khiadani, S. A. A. Mirjalily, and H. Kargarsharifabad, "A novel solar desalination system equipped with thermoelectric generator, reflectors and low-cost sensible energy-storage for co-production of power and drinking water," *Desalination*, vol. 567, Dec. 2023, Art. no. 116955.

SYED ZAHURUL ISLAM (Member, IEEE) received the Ph.D. degree in electrical power engineering from Universiti Putra Malaysia (UPM), Serdang, Malaysia, in 2016. Currently, he is a Senior Lecturer with the Department of Electrical Engineering, Faculty of Electrical and Electronic Engineering (FKEE), Universiti Tun Hussein Onn Malaysia (UTHM), Batu Pahat, Malaysia. He was also the Head of the Focus Group, Power Integration Systems. His research interests include photovoltaic cell and energy modeling, photovoltaic cooling, green energy for smart grid, smart city, energy efficiency management studies, and renewable and sustainable energy for community economic growth. He also practices as a professional technologist and a consultant in electrical and electronics engineering in a local consulting firm. He is also a Chartered Engineer and a Professional Technologist (P.Tech.) registered under the IET (U.K.) and MBOT (Malaysia), respectively, a member of IET (U.K.), IEEE (USA), IEEE Young Professionals, and IEEE Power and Energy Society (IEEE-PES). He is the Introducer and a current Advisor of UTHM IET On Campus for young engineers' professional development. He is the author or co-author of many articles, proceedings, and book chapters published in high impact factor journals and conferences. In IEEE conferences, journals, and other scientific publications, he serves as an invited reviewer. For more information visit the link (https://community.uthm.edu.my/zahurul).

ASMARASHID BIN PONNIRAN (Member, IEEE) received the bachelor's degree in electrical engineering from Universiti Tun Hussein Onn Malaysia (UTHM), the Master of Engineering degree in electrical—power from Universiti Teknologi Malaysia (UTM), and the Doctor of Engineering (Ph.D.) degree in energy and environmental science from Nagaoka University of Technology, Japan. He is currently a Professor with the Faculty of Electrical and Electronic Engineering, UTHM. His research interests include power electronics, particularly in converter design and optimization, modular multilevel converter switching strategies, high-power-density converters, high-voltage-gain converters, and high-frequency applications. His work is mainly directed toward renewable energy, electric vehicles, smart grid systems, and data centre power systems. For more information visit the link (https://community.uthm.edu.my/asmar).

MOHAMMAD RASHED M. ALTIMANIA received the Bachelor of Science degree in electrical engineering from Qassim University, in March 2010, the Master of Science degree in electrical engineering from The University of Tennessee at Chattanooga, in May 2014, and the Ph.D. degree in electrical engineering from Missouri University of Science and Technology, Rolla, MO, USA, in 2020. He is currently an Associate Professor with the Electrical Engineering Department, University of Tabuk, Tabuk, Saudi Arabia. His current research interests include modeling and design of power electronic converters, switched-capacitor converters, power and energy systems, renewable energy harvesting (wind and solar energy), smart grids, virtual power plants, distributed generations, and solar desalination.

KHALED SALEEM S. ALATAWI received the B.S. degree in electrical engineering from the King Fahd University of Petroleum and Minerals, Dhahran, Saudi Arabia, in 2008, and the M.S. and Ph.D. degrees in electrical engineering from the University of Denver, Denver, CO, USA, in 2013 and 2019, respectively. He is currently an Associate Professor with the Electrical Engineering Department, University of Tabuk, Tabuk, Saudi Arabia.

FAHAD M. ALMASOUDI received the M.S. and Ph.D. degrees in electrical engineering from the University of Denver, USA, in 2013 and 2018, respectively. He is currently an Associate Professor with the Department of Electrical Engineering, University of Tabuk, Tabuk, Saudi Arabia. His current research interests include renewable energy, power systems, smart grid, and modeling and control of power converters.

AMIMUL AHSAN received the Ph.D. degree in civil engineering from the University of Fukui, Japan, in 2009. Currently, he is an Associate Professor with the Department of Civil and Environmental Engineering, Faculty of Engineering and Technology, Islamic University of Technology (IUT), Gazipur, Bangladesh, and also an Adjunct Associate Professor with the Department of Civil and Construction Engineering, Faculty of Science, Engineering and Technology, Swinburne University of Technology (SUT), Melbourne, Australia. He was a Former Faculty Member (a Senior Lecturer; equivalent to an Assistant Professor) with the Department of Civil Engineering and a Key Researcher with the Institute of Advanced Technology (ITMA), University Putra Malaysia (UPM), Malaysia (2010–2017). He has nearly 20 years of research, teaching, and project experiences. He has published extensively in water and environmental engineering, including a few books and book chapters and over 100 journal articles. He has received a few international awards, including "Who's Who in the World 2015," "Leading Engineers of the World 2013," and the "Vice Chancellor Fellowship Award (Science and Technology)" from Sultan Selangor (Chancellor, UPM), in 2015. He is the Editor-in-Chief and the Founder of the *Journal of Desalination and Water Purification* and the *Journal of Advanced Civil Engineering Practice and Research*. He is involved with several collaborative research projects globally and has a Scopus H-index of 43. His specialization is environmental eng.- saline/surface water and wastewater treatments, solar water distillation, groundwater, rainwater, waste management, composting, landfill, sludge, air quality, and policy.

MOHAMMAD LUTFI OTHMAN (Senior Member, IEEE) received the B.Sc. degree (magna cum laude) in electrical engineering from The University of Arizona (UofA), Tucson, AZ, USA, in 1990, and the M.Sc. and Ph.D. degrees in electrical power engineering from Universiti Putra Malaysia (UPM), Serdang, Malaysia, in 2004 and 2011, respectively. He is currently an Associate Professor with the Department of Electrical and Electronic Engineering, Faculty of Engineering, UPM, where he is also a Research Member of the Advanced Lightning, Power and Energy Research (ALPER). He also practices as an electrical engineering consultant in electrical services installation works by diversifying as the electrical director/partner in a local engineering consulting firm. He is also a Professional Engineer (P.Eng.) registered under the Board of Engineers Malaysia (BEM), a Chartered Engineer (C.Eng.) registered under the Engineering Council, U.K., the Registered Electrical Energy Manager (REEM) under the Energy Commission Malaysia, and a Certified Professional in Measurement and Verification (CPMV) under Malaysian Green Technology Corporation. His research interests include power system protection (protective relay operation modeling and analysis, computational-intelligence-based data mining for knowledge discovery in relay database, application of artificial intelligence in protection algorithms, adaptive numerical protective relays, and development of numerical protective relays), power system operation (power quality, smart grid, and distributed generation), electrical services installation works (design and project administration consultancy), and energy efficiency management (demand side management, energy efficiency management, and building energy management systems).

JASIM UDDIN (Member, IEEE) received the M.Eng. (by Research) degree from International Islamic University Malaysia and the Ph.D. degree in electrical engineering from The Queensland University of Technology (QUT), Brisbane, Australia. He joined Cardiff Metropolitan University, U.K., as a Lecturer in electronics engineering with the Cardiff School of Technologies (CST), where he was later promoted as a Senior Lecturer. He currently leads the Electromagnetics, RF and Microwave (EM-RFMIC) Engineering Research Group. His research interests include electromagnetics, RF and microwave engineering, metamaterials, satellite communications, the IoT, and energy harvesting. He has been recognized as an Exceptional Global Talent by the Royal Academy of Engineering (RAE), U.K. He is a fellow of the Higher Education Academy (FHEA), a member of Engineers Australia (MIEAust), a member of the Institution of Engineering and Technology (MIET), and a Chartered Engineer (C.Eng.), U.K. Throughout his academic career, he has received several prestigious awards and scholarships, including the CSIRO Postgraduate Award, the University of Western Ontario Postgraduate Scholarship, the QUT Postgraduate Research Award (PRA), and the Higher Degree Research (HDR) Award. He has secured over £149 000 in competitive research funding from UKRI ILN+ Researchers in Residence (RiR), Ser Cymru, CSIRO, the Wales Innovation Network (WIN), and internal funds. His research contributions have been widely published, with over 60 technical papers in leading journals and international conferences. His work has appeared in IEEE Access, *IEEE Microwave Magazine*, *IET Microwaves, Antennas & Propagation*, *Microwave and Optical Technology Letters* (MOTL) (Wiley), *PLOS One*, *Energy Reports*, *Electromagnetics*, *Current Applied Physics*, *Journal of Crystal Growth*, and *Progress in Electromagnetics Research* (PIER).